Cabauw Data for the Validation of Land Surface Parameterization Schemes

ANTON C. M. BELJAARS* AND FRED C. BOSVELD

Royal Netherlands Meteorological Institute, De Bilt, the Netherlands

(Manuscript received 18 December 1995, in final form 17 September 1996)

ABSTRACT

This paper describes and interprets the 1987 data from Cabauw, the Netherlands, which can be used to test land surface schemes in stand-alone mode. The data are available from the authors for model development and research. It consists of half-hour averages of forcing data (wind, temperature, specific humidity at 20-m height, downward solar and thermal radiation, and precipitation) and validation data (net radiation, sensible heat flux, latent heat flux, ground heat flux, and soil temperature). To obtain a continuous time series of the forcing parameters and the surface energy fluxes, it was necessary to use a model to fill in the missing observations. The quality of the observations and the reliability of model data are assessed by exploiting the redundancy in the observations and by comparing the model output with the data when both are available. The monthly averages of sensible heat flux are believed to be accurate to within ± 5 W m^{-2} and the monthly means of net radiation and latent heat flux to within ± 10 W m^{-2}. An analysis of the evaporation data shows that evaporation from the interception reservoir is very common and that the canopy resistance can be modeled in terms of solar radiation, soil moisture, and atmospheric moisture deficit.

1. Introduction

The parametrization of land surface processes is an important aspect of numerical weather prediction and climate modeling. The main purpose of the land surface scheme in such models is to provide the atmosphere with surface fluxes of momentum, heat, and moisture. A wide variety of land surface schemes has been developed over the years (e.g., Deardorff 1978; Dickinson et al. 1986; Sellers et al. 1986; Abramopoulos et al. 1988; Noilhan and Planton 1989; see Garratt 1993 for a review), and all of them have been tested with the help of field data. Most of the validation studies concentrate on the diurnal cycle only and pay little attention to the seasonal timescale. The reason is that most field campaigns with observations of surface fluxes have a duration of only 1 or 2 months. It is only recently that more attention has been paid to longer timescales.

The Project for Intercomparison of Landsurface Parametrization Schemes (PILPS) is an initiative to intercompare schemes, with emphasis on the seasonal cycle of the surface energy fluxes (Henderson-Sellers et al. 1993, 1995). In phase 2a of the project, different schemes are compared in stand-alone mode by providing the atmospheric forcing from an observational time series. The advantage is that the differences between schemes can be assessed without interference from atmospheric feedbacks. This procedure was also followed by Viterbo and Beljaars (1995) to improve and test the land surface scheme in the European Centre for Medium-Range Weather Forecasts (ECMWF) model. Large-scale models operate simultaneously in different climate zones, and the land surface scheme must be able to cope with that. For a proper validation of land surface schemes, it is therefore necessary to have access to datasets that cover different climatological regimes.

The 1987 data from Cabauw, the Netherlands, were originally prepared to test the ECMWF scheme (Beljaars and Viterbo 1994), but was later also used as one of the first datasets in the PILPS project (Chen et al. 1997). The idea in PILPS was to start the intercomparison with a case in which the stress on evaporation from soil moisture was of secondary importance. The precipitation at Cabauw is spread rather uniformly over all seasons, and therefore drying out of the soil is a rare phenomenon. However, it is shown by Chen et al. (1997) that the differences between schemes in the intercomparison are still large. A discussion of possible causes for these differences is beyond the scope of this paper, but there are a number of questions that can be addressed from the data point of view. The first obvious question is, how were Cabauw data prepared and how accurate is the resulting dataset? It was already clear from the beginning that an inconsistency existed between the dif-

* Current affiliation: ECMWF, Shinfield Park, Reading, United Kingdom.

Corresponding author address: Fred C. Bosveld, Royal Netherlands Meteorological Institute, P.O. Box 201, 3730 AE De Bilt, the Netherlands.
E-mail: bosveld@knmi.nl

ferent radiation components necessary for the atmospheric forcing in models and the net radiation that is used to derive the latent heat flux (see Beljaars and Viterbo 1994). Therefore, some additional work was necessary to study the data problems. There are also other questions about the soil parameters, vegetation characteristics, etc.

This paper describes the further analysis of the 1987 Cabauw data, and a revised dataset is available now (it can be obtained from the authors). Three aspects have been improved over the original data as documented by Beljaars and Viterbo (1994): (i) an improved quality control scheme has been implemented, (ii) bias corrections have been applied to radiation and flux observations, and (iii) the procedure to fill in gaps with missing data has been improved.

The first purpose of this paper is to document the data, to document the procedures that were followed to correct biases and fill in gaps, and to address the accuracy issue. It will also show how datasets can be prepared even if the observation records are not complete. Such data activities are becoming increasingly important for the validation of weather and climate models. This paper concentrates on long timescales. Although the dataset itself consists of a time series of half hour averages, the emphasis in this paper is on the annual cycle, based on monthly averages, and its accuracy.

The second aim of this paper is to derive parameters from the observations that are relevant for parametrization in models and to interpret the results in the context of climate problems. One of the main questions that will be addressed is, how does the land surface regulate the moisture flux into the atmosphere? This will be done by analyzing the surface resistance for evaporation as a function of soil moisture, atmospheric moisture deficit, and radiation. Surface resistances for forest are widely studied (e.g., Jarvis 1976; Baldocchi et al. 1991), but much less is known about the characteristics of land surfaces with low vegetation [see Kim and Verma (1991) for an analysis of First Field Experiment (FIFE) data].

Long-term monitoring of surface fluxes is difficult, and therefore the climatology of sensible and latent heat fluxes based on observations is virtually nonexistent. Well-known field experiments such as the Hydrological Atmospheric Pilot Experiment (André et al. 1986), FIFE (Sellers et al. 1988), Amazonian Regional Micrometeorological Experiment (Shuttleworth et al. 1984), and EFEDA [European International Project on Climate and Hydrological Interactions between Vegetation, Atmosphere and Land Surface (ECHIVAL) Field Experiment in Desertification-Threatened Area; Bolle et al. 1993] have given a wealth of data for particular locations for a limited time period. In addition, the carbon cycle is studied more and more (Wofsy et al. 1993; Vermetten et al. 1994), but the available data are not nearly sufficient to cover all climatological regimes and all seasons. Existing climatologies are mainly based on models that use input from the operational meteorological network (the so-called SYNOP stations; e.g., Henning 1989).

At Cabauw a continuous boundary layer monitoring program has been running at the 200-m tower since 1986 (earlier measuring programs at Cabauw had a slightly different configuration). It is used for general forecasting, research, and model validation. The measuring program includes profiles of wind, temperature, and moisture up to 200 m, as well as all the components of the surface energy balance. The description is limited to parameters that are relevant to the validation of land surface schemes. Therefore, the profiles along the 200-m mast are not discussed, except for wind, temperature, and moisture at the 20-m level, which will be used as atmospheric forcing in stand-alone simulations. The 20-m level has been chosen because it was the observation level closest to the lowest ECMWF model level.

The different components of the radiative balance at the surface are measured with standard instruments. Direct eddy correlation fluxes of sensible and latent heat are not measured, and therefore these fluxes are inferred from other observations. Two basic techniques exist for deriving sensible and latent heat fluxes from wind, temperature, and moisture profiles: (i) the profile method, in which sensible and latent heat fluxes are derived from profiles with the help of flux–profile relationships, and (ii) the Bowen method, in which the net radiation minus soil heat flux is partitioned over sensible and latent heat flux with the help of the Bowen ratio from the temperature and moisture profiles. Because the profile method for temperature is the most robust from a technical point of view, we use it for the sensible heat flux and derive the latent heat flux as a residual of the surface energy balance. The method is compared with the Bowen method for the measuring periods in which the Bowen method is considered to be reliable.

For testing of a land surface scheme in stand-alone mode, it is necessary to have a continuous time series of the atmospheric forcing (i.e., wind, temperature, downward radiation, and precipitation). It is also desirable to have continuous records of the validation data (e.g., fluxes of sensible and latent heat) because it allows the computation of diurnal averages, monthly averages, etc. The observational material coming from Cabauw shows gaps due to instrument failure, problems with maintenance, and difficulties with the data communication. Short gaps are filled by interpolation; longer periods of missing data are filled with the help of the model by Van Ulden and Holtslag (1985). The model is used in two different ways—if the net radiation at Cabauw is still available, this observation is used as input to the model (model I), and otherwise standard SYNOP observations and solar downward radiation from the station in De Bilt, the Netherlands, are used as input to the model (model II). De Bilt is about 25 km away from Cabauw. The quality and impact of these procedures are discussed in the subsequent sections. Finally, an analysis

TABLE 1. Observed parameters used to produce the final data.

	Measuring height (m)	Instrument
Parameters (Cabauw)		
Wind (speed and direction)	20	Gill propeller vane 8002DX
Temperature difference	20 and 10	Thermocouple
Temperature difference	10 and 2	Thermocouple
Temperature difference	2 and 0.6	Thermocouple
Temperature	0.6	Thermocouple
Wet-bulb temperature difference	20 and 10	Thermocouple
Wet-bulb temperature difference	10 and 2	Thermocouple
Wet-bulb temperature difference	2 and 0.6	Thermocouple
Wet-bulb temperature	0.6	Thermocouple
Downward solar radiation	1.5	Kipp CM 11 pyranometer
Downward diffuse solar radiation	1.5	Kipp CM 11 (with shadow band)
Downward thermal radiation	1.5	Eppley radiometer
Upward thermal radiation	1.5	Eppley radiometer
Net total radiation	1.5	Funk
Soil heat flux	−0.05	TNO* heat flux transducers
Soil heat flux	−0.10	TNO heat flux transducers
Precipitation	0	KNMI** rain gauge
Soil temperature	0	Nickel resistance thermometer
Soil temperature	−0.02	Nickel resistance thermometer
Parameters (De Bilt)		
Wind (speed and direction)	10	Cup anemometer + vane
Temperature in screen	1.5	Platinum resistor
Relative humidity in screen	1.5	Hygromer element
Cloud cover	—	Estimated by observer
Precipitation	0	KNMI rain gauge
Actual weather (WW code)	—	Assessed by observer
Downward solar radiation	1.5	Kipp CM 11 pyranometer

* Netherlands Organization for Applied Scientific Research (TNO).
** Royal Netherlands Meteorological Institute (KNMI).

is made of the canopy resistance in terms of environmental variables.

2. The Cabauw measuring program

The measuring program that was operational in 1987 is described in more detail by Monna and van der Vliet (1987). Here, we concentrate on parameters and aspects that are most relevant to the validation of land surface schemes. The observational parameters used in this paper are summarized in Table 1.

a. Instrumentation

Radiation at the earth surface is at the core of the surface energy balance, and therefore it is important to consider the quality of the instruments. All the radiation instruments are standard ones, but are equipped with a ventilation system to prevent condensate from forming and to keep the temperature of the instruments close to the air temperature. The solar (Kipp) and net radiation instruments (Funk) are calibrated in the laboratory in the shortwave range against reference instruments. The reference instrument for solar radiation (Kipp) has been calibrated by the World Radiation Centre in Davos, Switzerland, and is assumed to be a correct standard to within a few percent. For the longwave instruments (Eppley) the manufacturer's calibration is used.

The reference net radiation instrument (Funk) has been calibrated by the Belgian Meteorological Institute. They distinguish a short- and a longwave calibration, but according to their report the longwave sensitivity is only 3% less than the sensitivity in the shortwave range. Operationally, the shortwave calibration is used for the Funk instrument. It should be realized, however, that Funk-type instruments suffer from two basic problems: (i) they have to operate simultaneously in the short- and longwave ranges, which implies a design compromise, and (ii) the transparency of the polyethylene domes suffers from aging, which results in less sensitivity of the instrument during normal operation than during calibration.

The other critical issue determining the quality of the sensible and latent heat fluxes is the accuracy of the vertical difference of dry- and wet-bulb temperatures. The temperature differences are measured with the help of thermocouples between nearby levels. At both ends (at 0.6 and 200 m) an absolute temperature is measured by a thermocouple using melting ice as a 0°C reference. The redundancy in the temperature chain is used to monitor drift. Amplifiers are adjusted when the sum of the temperature differences along the tower deviates systematically from the difference of absolute temperatures by more than 0.2°C. The temperature sensors (wet and dry) are double shielded and ventilated at a speed of

about 6 m s^{-1} to minimize radiation errors (Slob 1978). The accuracy of the measured temperature difference between levels is about 0.05°C. Long-term averages are better, as we will see later.

The wind observations at the 20-m level come from two auxiliary masts. The instrument with minimum flow distortion and wake effects is selected, dependent on wind direction.

b. Data reduction procedures and maintenance

All sensor signals are amplified and sampled every 3 s. Averages and standard deviations are computed over 10-min intervals, and the results are transmitted to the meteorological service in De Bilt. The 10-min averages are stored in a data archive, from which daily reports are produced for manual inspection. The archive is also cleaned automatically and manually by adding status information indicating which data points are believed to be suspect.

Maintenance is done on a regular basis. The routine maintenance schedule consists of weekly cleaning of radiation instruments, checking of water supply to the wet-bulb thermometers, and cleaning of the wet bulbs. In addition to the weekly schedule occasional repair work is carried out in response to observed problems from the daily reports. In the latter case, the response time is a few days at most.

From the 10-min data archive, a 30-min archive is created every month. The latter has fewer elements than the 10-min archive because a selection procedure is applied to the wind instruments (the instrument on the upstream boom is selected). The 30-min archive is the basis for the further analysis and data processing in this paper.

3. Measuring site

The tower is located in the center of the Netherlands (51°58′N, 4°56′E) at a distance of 1 km from the Lek River, one of the main branches of the Rhine. The surroundings are flat and consist of meadows and ditches with scattered villages, orchards, and lines of trees. The meadows are used for grazing and for the production of hay. The measuring field itself has grass that is kept at a height of about 8 cm by frequent mowing. The direct surroundings of the tower are free of obstacles up to a few hundred meters in all directions. For the predominant wind direction (southwest), the flow is unperturbed over an upstream distance of about 2 km.

In the context of the validation of a land surface parametrization scheme, it is necessary to know the terrain parameters that are relevant to the scheme. Not all parameters are known for Cabauw, but many have been documented in earlier studies (see Van Ulden and Wieringa 1996 for a review of research done with the Cabauw data). Albedo is documented by Duynkerke (1992) and is further discussed in section 4a as part of the procedure to check consistency in the radiation observations.

The aerodynamic roughness length of the direct surroundings of the terrain (within a radius of a few kilometers) is given by Beljaars (1988) and used for the calculation of fluxes in section 4d. However, the measuring location has been selected for unperturbed fetch, and therefore the typical ''regional'' roughness length (at scales of 10 km and up) is larger than the average, within a radius of a few kilometers. An effective roughness length of the area (one that produces a representative momentum flux for a large area in a model) is probably on the order or 0.1 m rather than 0.01 m, which is more typical for grassland.

The roughness length for heat is controversial and probably too simple as a concept. However, many models have this parameter, and most of them set it equal to the aerodynamic roughness length. It is well known now that the roughness length for heat is smaller than the one for momentum, and a one order of magnitude difference is probably a safe guess at this stage (Garratt and Francey 1978). Beljaars and Holtslag (1991) found indications from observations at Cabauw that the roughness length for heat is even smaller, due to the effects of heterogeneous terrain.

The information on the roughness lengths might suggest that the Cabauw site is very heterogeneous, but roughness parameters tend to be highly sensitive. The heterogeneity at Cabauw is limited to the momentum transfer and is due to scattered obstacles. There is no indication that sensible and latent heat fluxes are heterogeneous (see Beljaars 1982; Beljaars et al. 1983). This is confirmed, as we will see later, by the consistency between latent heat fluxes from the Bowen and the profile methods, which have different footprints.

The vegetation cover at Cabauw is close to 100% all year round. Even in winter, after mowing or after a dry spell it is unusual to see any bare soil. The leaf area index has never been measured, but it is considerably larger than one (for a leaf area index near one, the bare soil would be visible). Saugier and Ripley (1978) give typical values for natural grassland (not at Cabauw). They specify a leaf area index of 0.35 to 1.5 for the green leaves, dependent on season, and an index of 3 to 4.2 for the dead leaves. Subjective estimates of the dominant grass species at the measuring field are *Lolium perenne* (55%), *Festuca pratense* (15%), and *Phleüm pratense* (15%). The surrounding area is dominated by *Lolium perenne* (40%), *Poa trivialis* (20%), and *Alopecurus geniculatus* (10%). The mixture of grass species in this area has been selected for high yield under the given climatological conditions and for the given soil type.

a. Hydrologic soil properties

The soil characteristics for the Cabauw area were studied by Jager et al. (1976), with the help of laboratory

analysis of soil samples and a visual inspection of the soil profile in a 120-cm-deep profile pit. They describe the vertical structure as follows:

1) 0–3 cm is the turf zone;
2) 3–18 cm is 35%–50% clay (particles ≤ 2 μm) and 8%–12% organic matter with high root density;
3) 18–60 cm is 45%–55% clay (particles ≤ 2 μm and 1%–3% organic matter with low root density;
4) 60–75 cm is a mixture of clay and peat; and
5) 75–700 cm is peat.

Drainage of the terrain is through narrow parallel ditches, which are on average 40 m apart. The water level in the ditches is artificially maintained at about 40 cm below the surface. This keeps the peat layer and bottom part of the clay always saturated. The height of the water table in the soil depends on the distance from the nearest ditch. It can be very close to the surface after abundant rain and can go down to the top of the peat layer after a dry spell.

Physical soil properties are important for the parametrization of hydrology in land surface schemes. We use the soil type classification for the Netherlands proposed by Wösten et al. (1994) because the physical properties of their soil classes are well documented on the basis of many soil samples taken in the Netherlands. The soil types that are close to the texture description given above are the upper-soil type B11 (fairly heavy clay; top 18 cm) and the deep soil types O12 (fairly heavy clay; between 18 and 60 cm) and O16 (peat; below 75 cm). The soil properties that correspond to these soil types are given by Wösten et al. (1994) on the basis of a large number of samples. The water retention curves and conductivity curves are fitted with the empirical relations proposed by Van Genuchten (1980; see Fig. 1 and Table 2). The second source of information is the study by Jager et al. (1976). They analyzed soil samples taken at Cabauw at three locations at depth intervals of 10 cm, and concluded that the 60-cm-deep clay layer has fairly uniform characteristics. The averaged water retention curve from all the clay samples taken by Jager et al. (1976) is reproduced in Fig. 1a. Correspondence with the Wösten et al. (1994) clay types is good at low potentials, but it should be realized that the uncertainty in the curves from individual samples is large. We also think that the analysis by Wösten et al. (1994) is more accurate because it is done with more recent technology and based on a larger number of samples.

Common parameters derived from the water-retention curves are the permanent wilting point θ_{pwp} and the the field capacity θ_{fcp}, defined as the volumetric water content at matric potentials of 16 000 hPa and 250 hPa, respectively (Wösten et al. 1994). For soil type O12, $\theta_{pwp} = 0.253$ m^3 m^{-3} and $\theta_{fcp} = 0.468$ m^3 m^{-3}. This makes the water-holding capacity of a 70-cm-deep clay layer equal to $0.7(0.468 - 0.253) = 0.15$ m, which is also the value used by Manabe (1969) and in most bucket models since.

b. Thermal soil properties

The thermal properties of the soil in Cabauw have never been studied from laboratory soil samples, but it is possible to infer the thermal conductivity κ and the volumetric heat capacity C from the diurnal cycle of the soil heat flux G and that of the soil temperature T_S, assuming that the diffusion for a homogeneous medium applies (e.g., Hillel 1982):

$$C\frac{\partial T_S}{\partial t} = \kappa\frac{\partial^2 T_S}{\partial z^2}. \tag{1}$$

For a single frequency ω, the solution reads

$$T_S = \hat{T}e^{i\omega t}, \qquad G = \hat{G}e^{i\omega t}, \tag{2}$$

$$\hat{T} = \hat{T}_0 e^{-(i+1)z/d}, \qquad d = \left(\frac{2\kappa}{\omega C}\right)^{1/2}, \tag{3}$$

and

$$\hat{G} = \kappa\frac{\partial \hat{T}}{\partial z} = (i + 1)d^{-1}\hat{T}_0 e^{-(i+1)z/d}, \tag{4}$$

where $\hat{T}$ and $\hat{G}$ are complex amplitudes, with $\hat{T}_0$ being the complex amplitude of temperature at the surface ($z = 0$). The solutions apply to any Fourier component, but for the analysis here we limit to the diurnal cycle [$\omega = 2\pi\,(24\text{ h})^{-1}$] because this is the Fourier component with the largest amplitude. From the observations of the heat flux at 5 cm and 10 cm deep and the temperature at 2 cm deep, we compute the amplitude and phase of the diurnal cycle, denoted by $|\hat{G}_5|$, $|\hat{G}_{10}|$, $|\hat{T}_2|$, ϕ_{G_5}, $\phi_{G_{10}}$, and ϕ_{T_2}, respectively. The penetration depth d, the thermal conductivity κ, and the volumetric heat capacity C are derived in the following way:

$$d = -0.05/\ln\frac{|\hat{G}_{10}|}{|\hat{G}_5|} = -0.05/(\phi_{G_{10}} - \phi_{G_5}), \tag{5}$$

$$\kappa = \frac{|\hat{G}_5|de^{(0.05-0.02)/d}}{\sqrt{2}|\hat{T}_2|}, \tag{6}$$

and

$$C = \frac{2\kappa}{\omega d^2}. \tag{7}$$

These parameters have been computed from the complex amplitudes of the diurnal cycles G_5, G_{10}, and T_{S_2} for every day in 1987, provided that sufficient data are available, that the absolute amplitudes of the two soil heat fluxes are larger than 2 W m^{-2}, and that the amplitude of T_{S_2} is larger than 1 K. The results are shown in Figs. 1c–e as time series of daily values, where the phase differences have been used for the penetration depth in Eq. (5) rather than the amplitudes because the latter gave noisier results.

Typical values of d, κ, and C are tabulated by Hillel (1982, using work by De Vries 1963) for clay with volumetric soil moisture contents of 0, 0.2, and 0.4 m^3 m^{-3}. The numbers for $\theta = 0.2$ and 0.4 (covering the range between the permanent wilting point and field capacity) are $d = 0.124$ and 0.122 m, $\kappa = 1.17$ and 1.59 W m^{-1} K^{-1}, and $C = 2.09$ and 2.93 M J m^{-3} K^{-1}, respectively. Comparing these typical numbers with the results of the analysis of diurnal cycles in Figs. 1c–e, we see that the penetration depth d is very similar, but that the ''observed'' κ and C are systematically lower than the typical values given by Hillel. Whether this should be attributed to problems with the observations, to vertical heterogeneity of the soil, or to differences between the clay type used by Hillel and the actual soil in Cabauw is not clear at this stage.

4. Data processing

The data processing starts from the cleaned archive with half hour averages of observations and has a series of steps that are described in the following subsections. The basic philosophy is to keep as much as possible of the original data and to rely on synthetic data only if absolutely necessary. On the other hand, we tried to maintain accuracy and reliability by checking on internal consistency and by applying bias corrections if necessary.

a. Albedo

Unfortunately, albedo has not been measured on a routine basis, and it is therefore not included in the dataset. However, an estimate of the albedo is necessary to allow a consistency check on the radiation instruments. Albedo has been measured during campaigns and is documented by Duynkerke (1992) for the Cabauw location. He proposes the following dependency on solar elevation:

$$\mathrm{ALB} = 0.33 - 0.13 \sin\phi, \tag{8}$$

where ϕ represents the solar elevation. This relation was derived from observations in clear-sky conditions, when the downward solar radiation is dominated by direct radiation from the sun. For diffuse radiation with a uniform distribution over the angle of incidence, the albedo resulting from Eq. (8) is 0.2433. For non-clear-sky conditions, an empirical interpolation between the albedos for direct and diffuse radiation is based on the observation of the downward solar radiation SR_d and the diffuse downward solar radiation SRD_d from an instrument equipped with a shadow band:

$$\mathrm{ALB} = 0.33 - 0.13 \sin\phi - \left(\frac{\mathrm{SRD}_d}{\mathrm{SR}_d} - 0.1\right) \times (0.0867 - 0.13 \sin\phi). \tag{9}$$

Equation (9) reduces to Eq. (8) for clear-sky situations when the diffuse radiation is about 10% of the total downward solar radiation. The quality of this estimate as a function of SRD_d/SR_d has not been investigated, but the result is not very sensitive to the choice of parameters. The estimate of the albedo is believed to be accurate to within a few percent.

b. Radiation bias corrections

When testing a land surface scheme in stand-alone mode, downward solar and thermal radiation observations are used directly for the atmospheric forcing. In the current dataset, the latent heat flux is computed as a residual of the surface energy balance, and therefore the net radiation is also a very crucial parameter. It has already been noted by Beljaars and Viterbo (1994) that an inconsistency existed between the observed components of the radiation and the net radiation. Unfortunately, the upward solar radiation was not measured on a routine basis, and therefore a rigorous consistency check on instruments is not possible during the daytime. However, it is felt that the albedo estimate given in the previous section is reasonably accurate, and therefore consistency between instruments can be assessed to within a few percent.

Figure 2a shows a scatterplot of the sum of the radiation components as a function of net radiation. The mean slope deviates considerably from one with the largest error in slope for negative net radiation. This suggests that the instrumental problems in the longwave range are different from the ones in the shortwave range. The difference in sensitivity between the sum of the upward- and downward-facing longwave instruments and the net radiation instrument is clear from Fig. 2b, in which data points are used with negligible shortwave radiation (nighttime) for the month of June. A linear regression on the longwave radiation for the entire year of 1987 indicates that the sum of the two longwave components has an offset of 4 W m^{-2} and is 23% more sensitive than the net radiation instrument. We now make the sum of the longwave components compatible with the net radiation instrument by subtracting 4 W m^{-2} and by dividing it by 1.23. The scatterplot in Fig. 2c [$\mathrm{SR}_d(1 - \mathrm{ALB})$ as a function of $Q_n - (\mathrm{TR}_d - \mathrm{TR}_u - 4)/1.23$] indicates the difference in sensitivity in the shortwave range between the solar radiation instrument (Kipp) and the net radiation instrument (Funk). The mean slope for the entire year of 1987 is 1.16. The sensitivity difference has also been computed month by month and varies between 1.17 and 1.30 (1.23 for all months) for the longwave radiation, and between 1.12 and 1.32 (1.16 for all months) for the shortwave radiation. No obvious correlation exists between the ratios in the short- and the longwave range.

It is clear from these diagnostics that the differences between instruments have a systematic component and a variable component that varies from month to month. Some of the latter could be traced back to changes in

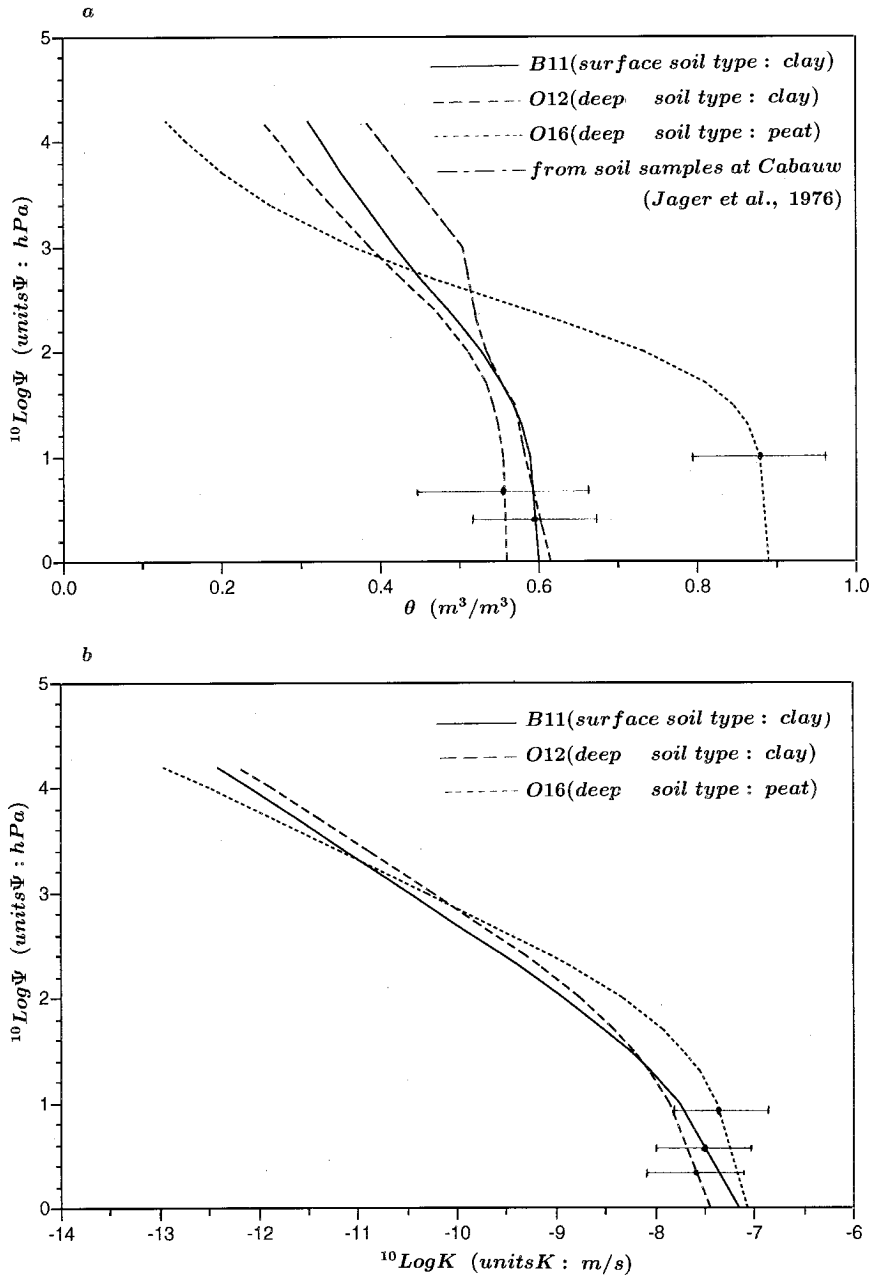

FIG. 1. Physical soil properties. (a) and (b) Water retention and soil water conductivity curves for surface soil type B11 (fairly heavy clay) and deep soil types O12 (fairly heavy clay) and O16 (peat), which are characteristic for the Cabauw area. The dash–dotted curve in (a) is the average from soil samples taken at three locations and at 10-cm-depth intervals down to a depth of 60 cm of the clay layer at Cabauw (Jager et al. 1976). The horizontal error bars indicate the spread of curves found by Wösten at al. (1994) from individual soil samples. (c)–(e) Time series of daily values of penetration depth d, soil conductivity κ, and volumetric heat capacity C, as derived from the diurnal cycle of observed soil heat fluxes and soil temperature.

the transmission of the polyethylene domes that protect the sensitive surfaces of the net radiation instrument (Funk). The domes were, for instance, replaced on 1 July, which gave an instantaneous jump in the mismatch between the sum of components and the net radiation. Indeed, the sensitivity ratio in the shortwave range between the solar instrument (Kipp) and the net radiation instrument (Funk) is 1.12 for the month of July, which is the lowest value for the entire year. The impact of the transmission change of the Funk domes in the longwave range is not known.

From the analysis above it is not clear which instru-

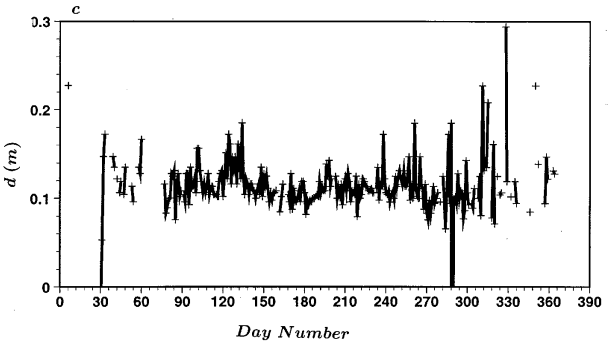

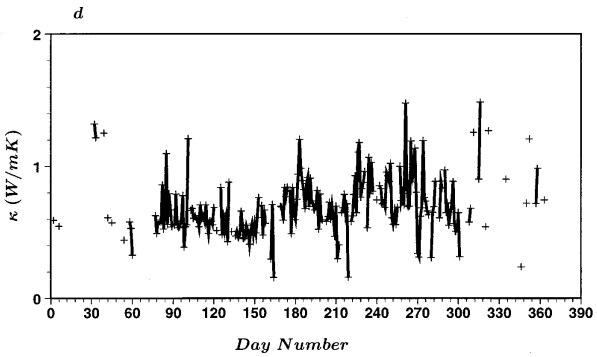

FIG. 1. (*Continued*)

ment has to be corrected. However, the aging of the Funk domes and the study by Halldin and Lindroth (1992) clearly suggest that the net radiation instrument is to blame for the bias in the shortwave radiation. The shortwave instrument is also much more standard and does not have the design compromises necessary to operate for both short- and longwave radiation. We therefore choose to increase the readings from the net radiation instrument by a factor 1.16, which makes the shortwave radiation as measured by the net radiation instrument consistent with that from the solar instrument for the annual mean of 1987.

The difference between downward and upward longwave radiation ($TR_d - TR_u$) has an offset, which was rather arbitrarily attributed to an offset in TR_d. However, the correction factor of 1.16 applied to the net radiation is not sufficient to compensate the difference in sensitivity between Q_n and $TR_d - TR_u$. In this case, there is no real reason to suspect either of the two. The study by Halldin and Lindroth (1992) suggests that the Funk instrument is indeed less sensitive in the longwave range than in the shortwave. We therefore increase the net radiation (Funk) by 6% of the net longwave radiation. The corrections read

$$TR_d^c = TR_d - 4 \tag{10}$$

and

$$Q_n^c = 1.16Q_n + 0.06(TR_d^c - TR_u), \tag{11}$$

where superscript c indicates the corrected parameter.

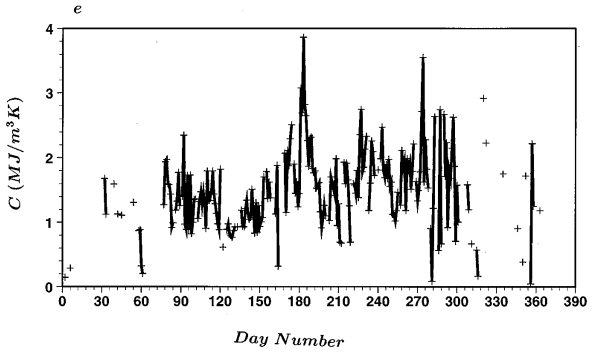

FIG. 1. (*Continued*)

The consistency of the radiation instruments on a monthly mean basis is illustrated in Fig. 3. The monthly mean residual of the radiation is much closer to zero after correction, but is still about 4% of the net radiation in summer. The difference between June and July is interesting because it reflects the effect of the replacement of the polyethylene domes of the Funk instrument on 1 July. The remaining inconsistency between radiation instruments varies from month to month, but is smaller than about ± 5 W m^{-2} for the monthly means.

c. Temperature bias corrections

The sensible heat flux is derived with the help of the so-called profile method, in which vertical temperature differences play a crucial role. Temperature differences are measured directly between heights of 0.6 and 2 m, and between 2 and 10 m. The total difference between 0.6 and 10 m is used in the profile method for sensible heat flux. The wet- and dry-bulb temperature differences between 0.6 and 2 m are used for the Bowen method. Fluxes from the Bowen method are not included in the

TABLE 2. Van Genuchten parameters of surface soil type B11 (fairly heavy clay) and deep soil types O12 (fairly heavy clay) and O16 (peat), according to Wösten et al. (1994). Types B11 and O12 apply to the top 18 cm and the layer from 18 to 60 cm, respectively. The parameters correspond to the empirical forms

$$\theta = \theta_r + \frac{\theta_s - \theta_r}{(1 + |\alpha\Psi|^n)^{1-1/n}} \tag{T1}$$

and

$$K = K_s \frac{[(1 + |\alpha\Psi|^n)^{(1-1/n)} - |\alpha\Psi|^{n-1}]^2}{(1 + |\alpha\Psi|^n)^{(1-1/n)(l+2)}}, \tag{T2}$$

where θ is volumetric soil water content (m^3 m^{-3}); θ_s is θ at saturation; θ_r is a reference θ; Ψ is the matric potential (hPa); K is hydraulic conductivity (m s); K_s is the value of K at saturation; and α, n, and I are empirical coefficients.

Type	θ_r (m^3 m^{-3})	θ_s (m^3 m^{-3})	K_s (10^7 m s)	α (hPa^{-1})	I (−)	n (−)
B11	0.00	0.60	6.09	0.0243	−5.395	1.111
O12	0.00	0.56	1.32	0.0095	−4.171	1.159
O16	0.00	0.89	1.24	0.0103	−1.411	1.376

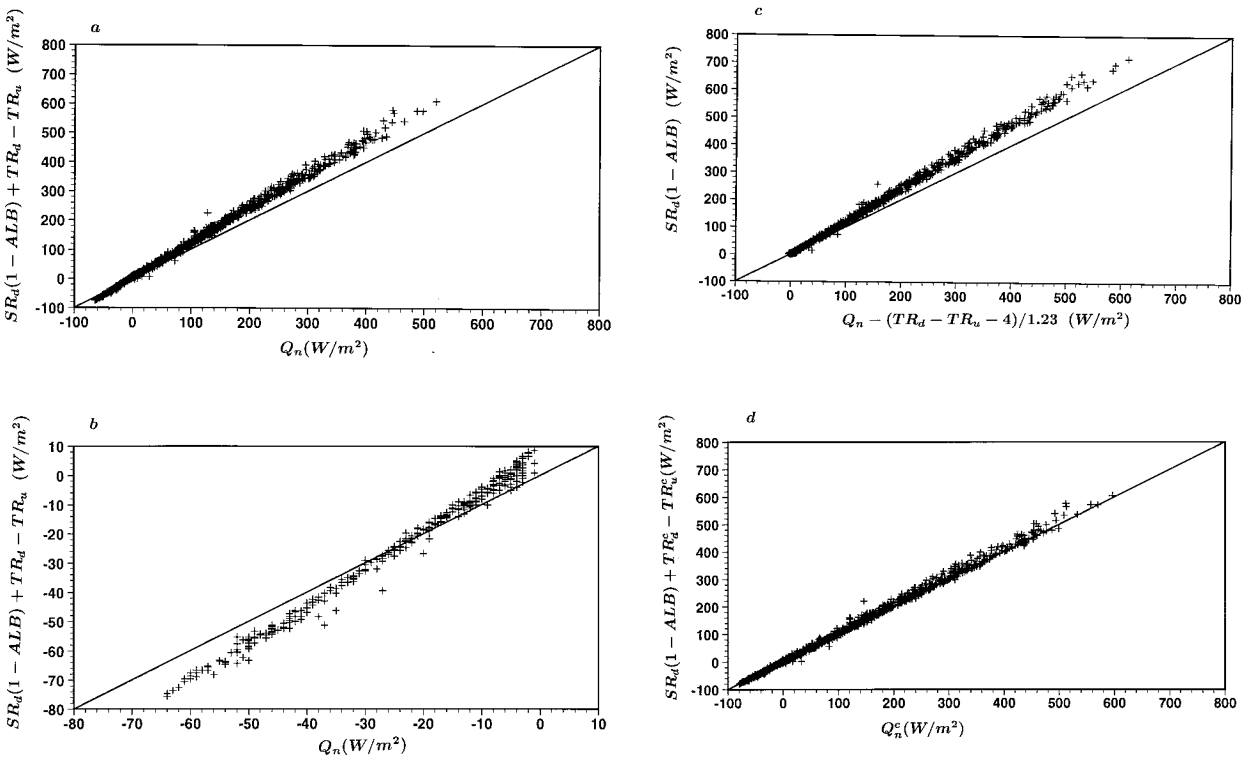

FIG. 2. Scatterplot of the sum of the radiation components against the net radiation for the month of June 1987. (a) Uncorrected data. (b) Nighttime or thermal radiation data only. (c) The solar part only. (d) Similar to (a) but after correction of the data.

final dataset because the method is not robust enough to provide good data coverage. The results from the Bowen method are used in this paper as an independent check on the profile method. Such a comparison also includes a check on representativeness because the 0.6–2-m differences used in the Bowen method have a smaller ''footprint'' than the 0.6–10-m temperature difference used in the profile method.

The Bowen method and the profile method rely heavily on small vertical temperature differences, and therefore it is important to make an estimate of the long-term stability of the temperature system. The differences are measured directly with thermocouples after amplification with low drift chopper amplifiers. The stability of the system is checked by considering the zero crossings of the dry- and wet-bulb potential temperature differences, defined in the following way:

$$\Delta\theta = \Delta T + \Gamma\Delta z \tag{12}$$

and

$$\Delta\theta_w = \Delta T_w + \frac{\gamma}{S+\gamma}\Gamma\Delta z, \tag{13}$$

where ΔT and ΔT_w are the dry- and wet-bulb temperature differences, Γ is the dry adiabatic lapse rate, Δz is the height difference over which the temperature difference is measured, $\gamma = C_p/\lambda$ is the psychrometer constant, C_p is the specific heat at constant pressure, λ is the latent heat of vaporization, and S is the derivative of the saturation specific humidity function with respect to temperature.

The interesting properties of $\Delta\theta_w$ are that it depends on the wet-bulb difference only and that it is proportional to $H_0 + \lambda E$, and therefore also to $Q_n - G_0$. Figure 4a shows $\Delta\theta_w$ between 0.6 and 2 m and between 2 and 10 m as a function of $Q_n - G_0$ for the month of June. These plots were made for all months, and from the month to month variation in the zero crossing it was concluded that the long-term stability of the temperature differences is within ± 0.02°C.

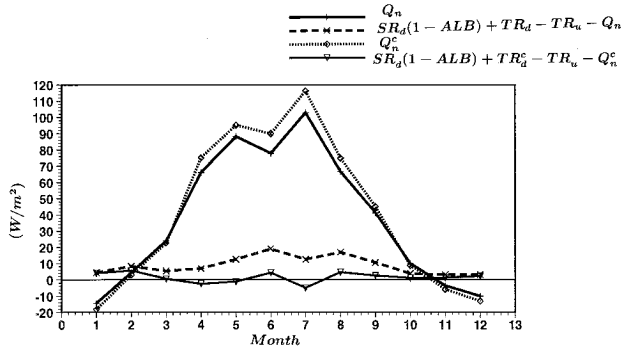

FIG. 3. Monthly mean net radiation and energy residual between the sum of components and net radiation before and after correction.

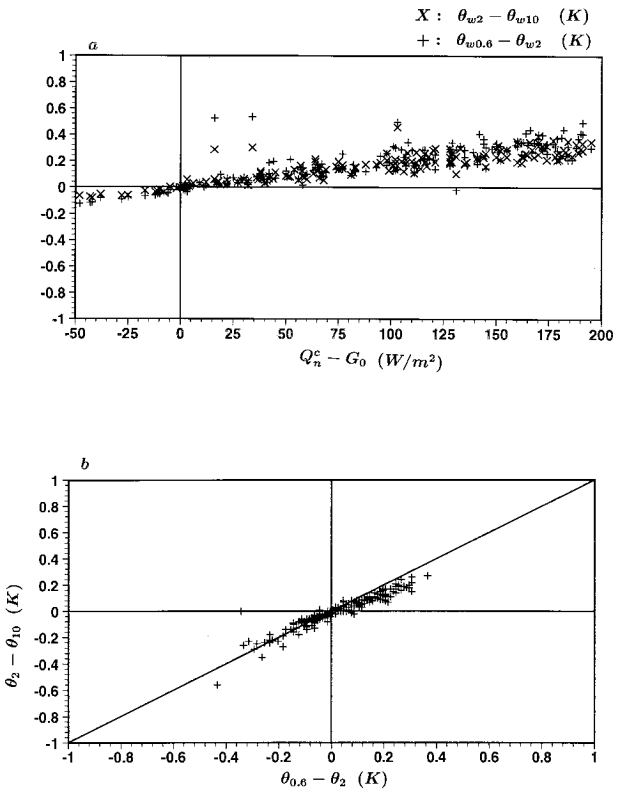

FIG. 4. (a) Wet-bulb potential temperature difference between 0.6 and 2 m (+) and between 2 and 10 m (×) as a function of net radiation minus ground heat flux, and (b) potential temperature difference between 2 and 10 m as a function of the difference between 0.6 and 2 m.

The dry-bulb temperature differences were checked by plotting the 0.6–2-m difference against the 2–10-m difference. It is assumed that both differences are proportional to the heat flux, and therefore they should cross zero at the same time.

Initially the wet-bulb temperature difference between 2 and 10 m showed a constant offset of 0.1 K from January to September. On 18 October, the thermocouple amplifier was adjusted and the offset disappeared. A correction was applied for this offset. Similarly, a persistent inconsistency of 0.03 K existed between $\theta_{0.6} - \theta_2$ and $\theta_2 - \theta_{10}$. The decision about which amplifier was to blame was based on a $\sigma\Delta T$ versus $\Delta\theta$ plot (standard deviation of temperature difference as a function of the vertical potential temperature difference), which is assumed to have a minimum at $\Delta\theta = 0$. The data points in Fig. 4 are the ones after corrections have been applied.

d. Fluxes from profiles

The procedure to derive sensible heat fluxes (H_0) from profile measurements is standard in principle. Wind gradients and potential temperature gradients are combined with surface-layer similarity functions for the surface layer, and fluxes of heat and momentum are computed iteratively (Nieuwstadt 1978). For Cabauw, the situation is a little more complicated because the fetch is not good enough to allow the use of the profile method in a standard way (Beljaars 1982; Beljaars et al. 1983). We know that the flux profile relationships are perturbed due to the effects of heterogeneous terrain. Therefore, we use a modified profile method in which the aerodynamic roughness length is specified from a site-specific table. This table is specified from an analysis of the standard deviation of horizontal wind (Beljaars 1988) and reproduced in Table 3. As input to the profile method we use wind speed at 10-m height, roughness length (dependent on wind direction; see Table 3), and temperature difference between 0.6 and 10 m. With the help of H_0 from the profile method, we also compute the latent heat flux from the surface energy balance: $\lambda E = Q_n - G_0 - H_0$. This is called the balance method for latent heat.

The Bowen method does not suffer from perturbations in the flux profile relationships because the only assumption is that the diffusivities for heat and moisture are the same. However, the method is less robust, as it relies on wet-bulb temperature measurements and has difficulties with Bowen ratios near -1. Here, we only use it to assess the quality of the profile fluxes. For the half hour intervals with reliable Bowen observations we compare the profile method for H_0 and the balance method for λE with the Bowen method for H_0 and λE. Figures 5a,b show scatterplots for the month of June of the profile and balance methods against the Bowen method.

The correlation between H_0 from the profile method and the Bowen method is very good for daytime, but a small bias exists for the nighttime observations. It is important to note that the profile method for H_0 is to a large extent independent of the Bowen method, and therefore this comparison is an important quality control on the profile method. The correlation between λE from the balance method and the Bowen method is even bet-

TABLE 3. Effective roughness length (in m), representative of a few kilometers of upstream terrain from the Cabauw tower for 18 wind direction classes (Beljaars 1988).

Direction	0–20	20–40	40–60	60–80	80–100	100–120	120–140	140–160	160–180
Summer	0.06	0.08	0.10	0.15	0.15	0.15	0.11	0.08	0.04
Winter	0.04	0.05	0.05	0.07	0.10	0.12	0.02	0.02	0.02
Direction	180–200	200–220	220–240	240–260	260–280	280–300	300–320	320–340	340–360
Summer	0.04	0.04	0.04	0.07	0.06	0.06	0.06	0.05	0.05
Winter	0.03	0.03	0.02	0.04	0.03	0.03	0.04	0.04	0.03

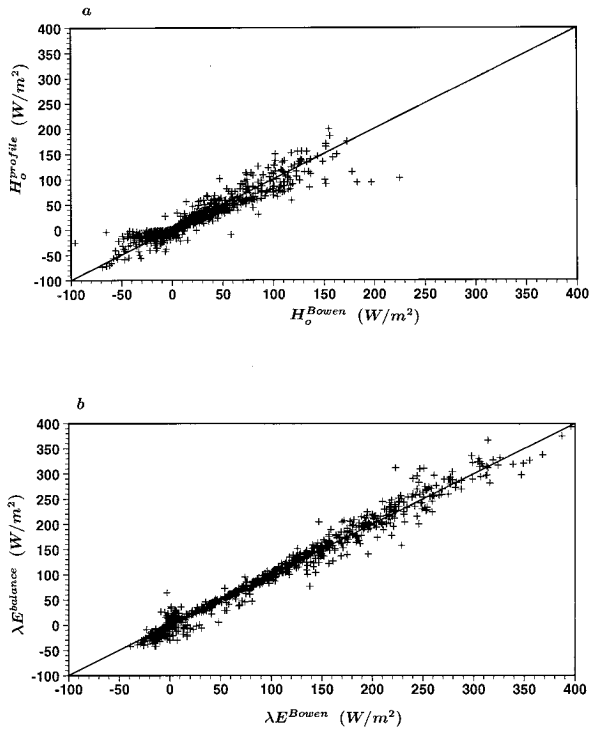

FIG. 5. (a) and (b) Comparison of the profile sensible heat and the balance latent heat flux against the Bowen fluxes (a) and (b) as scatterplots for the month of June and (c) as monthly mean differences.

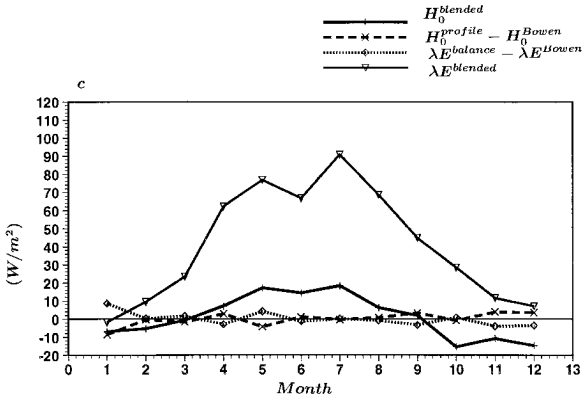

FIG. 5. (*Continued*)

ter, but this is not surprising. The balance method for λE and the Bowen method use the same radiation observation as input, and the net radiation dominates λE.

The monthly mean comparison of profile H_0 and balance λE on one hand and the Bowen data on the other hand is given in Fig. 5c. Data points for which both methods exist are used only in this comparison. The results of the comparison for months 1, 2, and 12 have less than 50% of data points, and are therefore less reliable. The maximum monthly mean difference between Bowen method and profile method is 4.5 W m^{-2} for sensible, as well as latent, heat flux. The main part of this difference is probably due to the Bowen method because it is more sensitive to biases in the temperature system. The sensitivity of the profile method for H_0 to systematic offsets in the temperature difference is 0.5 W m^{-2} per 0.01° offset in $T_{0.6} - T_{10}$. The sensitivity of the Bowen method for H_0 to a systematic bias in the wet-bulb temperature difference and the dry-bulb difference (simultaneously with opposite sign) is between 1.1 and 2.2 W m^{-2} per 0.01° offset. The maximum monthly mean error in $T_{0.6} - T_{10}$ is estimated to be 0.04°, resulting in a maximum bias of 2 W m^{-2} for the monthly mean sensible flux. On the annual timescale, there is no indication of a systematic bias.

e. Ground heat fluxes

The ground heat fluxes are measured at depths of 5 and 10 cm with heat flux transducers. To reduce the effects of possible soil heterogeneities, two sets of three transducers are used and the signals are averaged over the three observations. It is impossible to measure the soil heat flux at the surface directly. Therefore, the heat flux into the soil G_0 is inferred from either the temperature differences between 0 and 2 cm deep ($T_{S_0} - T_{S_2}$) or from extrapolation of G_5 and G_{10}.

The method that uses the temperature difference is called the Λ method because it uses the thermal conductivity between 0 and 2 cm deep to derive the heat flux from the temperature difference. Parameter Λ_s is calibrated for every day by making the amplitude of the diurnal cycle (first Fourier component $\hat{G}_0$) of G_0 equal to that of $\Lambda_s(T_{S_0} - T_{S_2})$. The diurnal amplitude $\hat{G}_0$ is computed from $\hat{G}_5^2/\hat{G}_{10}$ on the basis of the solution of the diffusion equation for a homogeneous medium. By computing Λ_s in this way, the possible effects of nonrepresentative soil properties near the temperature sensors are automatically taken care of. The procedure is similar to the one described by De Bruin and Holtslag (1982), and has the advantage that the rapid changes in the soil heat flux (say, on a half hour timescale) are well represented by the temperature differences and that the slow variations are constrained by the soil heat fluxes at depths of 5 and 10 cm.

The second method is the Fourier method. The time series of G_5 and G_{10} are transformed to Fourier space, and the Fourier components are extrapolated to the surface and backtransformed to obtain a time series for G_0. The method uses a maximum of 10 Fourier components to represent the diurnal cycle. If a particular Fourier component has an amplitude of below 1 W m^{-2} at a depth of 10 cm, or if the amplitude at 5-cm depth is larger than two times the amplitude at 10-cm depth, then the amplitude and phase of the Fourier component of G_5 are copied and no extrapolation is done.

Both methods give very similar results. The only difference is that the Fourier method does not reproduce the rapid changes at the surface because these changes do not penetrate to the 5- or 10-cm levels and are therefore not seen by the observations.

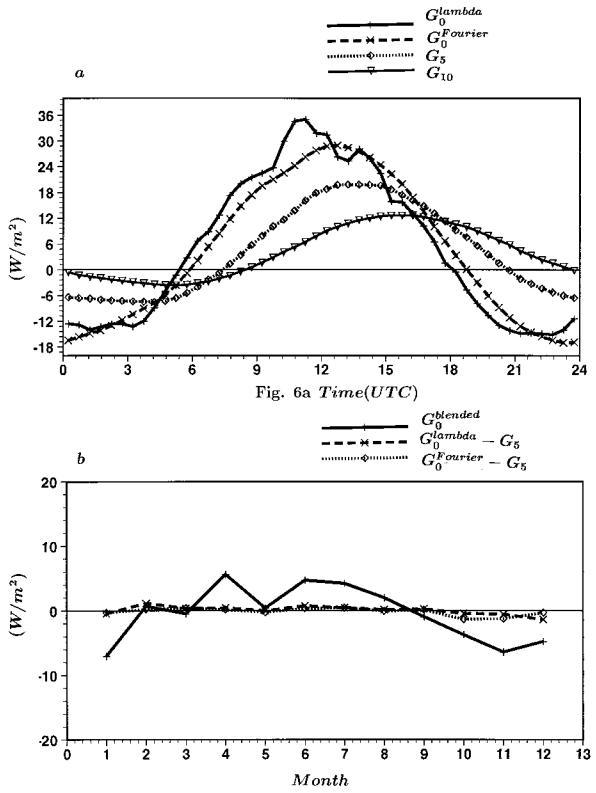

FIG. 6. Comparison of ground heat flux at the surface with the Λ method and the Fourier method, and the observed fluxes at depths of 5 and 10 cm. (a) The averaged diurnal cycle for the month of June. (b) Monthly mean differences between methods for 1987.

An example of an averaged diurnal cycle of the ground heat flux at three depths is given in Fig. 6a. Monthly mean differences between G_0 from both methods and G_5 are reproduced in Fig. 6b for comparison with the monthly means of G_0. We see that the monthly mean soil heat flux varies between -7 W m^{-2} and $+6$ W m^{-2}, with a vague hint of an annual cycle. It is difficult to make an estimate of the monthly mean error of this parameter, but given the differences between instruments, it is expected to be less than 1 W m^{-2}.

f. Synthetic data

The time series of half-hourly observations from Cabauw is not continuous. Interruptions do occur due to maintenance, instrument failure, errors in data communication, and the manual ''suspect'' flagging after the observation has been archived. The wet-bulb measurements have a lower coverage than the other observations because of incidental problems with the water supply and because of freezing in winter. To make the time series continuous, missing data are added by interpolation for gaps shorter than 2 h and by using a model in combination with either radiation data from Cabauw (if available) or SYNOP data from De Bilt (25 km from Cabauw).

TABLE 4. Parameters in the final dataset. All parameters except YYMMDD, HHMN, G_5, G_{10}, T_{S0}, and T_{S2} have selection indicators for every half hour interval. The selection indicator can be 0, 1, or 2 and is used to indicate how the parameter for that particular half hour interval has been obtained; 0 is used for measurements, 1 means that the parameter is coming from model I (the basic input is net radiation measured in Cabauw), and 2 means that model II has been used (the model has been used with input from SYNOP station at De Bilt). Here, G_0 can also have indicator code -1 or -2. Indicator code -1 means that the Fourier method has been used instead of the Λ method, and code -2 means that G_5 has been copied. RAINL and RAINC share a single indicator code; the partitioning of observed precipitation between large-scale and convective precipitation is made on the basis of the WW actual weather code from the SYNOP message in De Bilt. The parameters G_5, G_{10}, T_{S0}, T_{S2}, and SRD_d can have missing data, which are flagged by -9999. The thermometers that measure T_{S0} and T_{S2} are buried in the soil and should therefore not be confused with the surface radiation temperature.

Parameter identification	Units	Description
YYMMDD		Date (e.g., 870701 for 1 July 1987)
HHMN	UTC	Time (e.g,. 1015 for 30 min between 1000 and 1030)
F_{20}	m s^{-1}	Wind speed at 20-m height
D_{20}	deg	Wind direction at 20-m height
T_{20}	C	Temperature at 20-m height
Q_{20}	g Kg^{-1}	Specific humidity at 20-m height
$S\,R_d$	W m^{-2}	Downward solar radiation
$T\,R_d$	W m^{-2}	Downard thermal radiation
RAINL	mm	Large-scale precipitation
RAINC	mm	Convective precipitation
UST	m s^{-1}	Friction velocity
H_0	W m^{-2}	Sensible heat flux
ΛE	W m^{-2}	Latent heat flux
$T\,R_u$	W m^{-2}	Upward thermal radiation
Q_n	W m^{-2}	Net total radiation
G_0	W m^{-2}	Ground heat flux at the surface
G_5	W m^{-2}	Ground heat flux at 5-cm depth
G_{10}	W m^{-2}	Ground heat flux at 10-cm depth
T_{S0}	C	Soil temperature 0-cm depth
T_{S2}	C	Soil temperature 2-cm depth
SRD_d	W m^{-2}	Downward diffuse solar radiation

1) FORCING PARAMETERS

In order to make the wind from De Bilt at 10-m height compatible with the 10-m wind at Cabauw, exposure correction is applied according to Wieringa (1986). It implies a logarithmic extrapolation from 10 m upward, using information on the roughness length for the De Bilt station, and a downward interpolation to 10 m at Cabauw, using the roughness lengths of Table 4. Wieringa proposes an extrapolation height of 60 m, but in order to get an unbiased estimate for Cabauw, an extrapolation height of 500 m is used here. The other observations (temperature, humidity, wind direction, solar radiation, and cloud cover) are directly used as if they were made in Cabauw. Wind at 10 m, temperature, and specific humidity at 2 m are all extrapolated to 20 m with the help of the dimensionless profile functions proposed by Beljaars and Holtslag (1991).

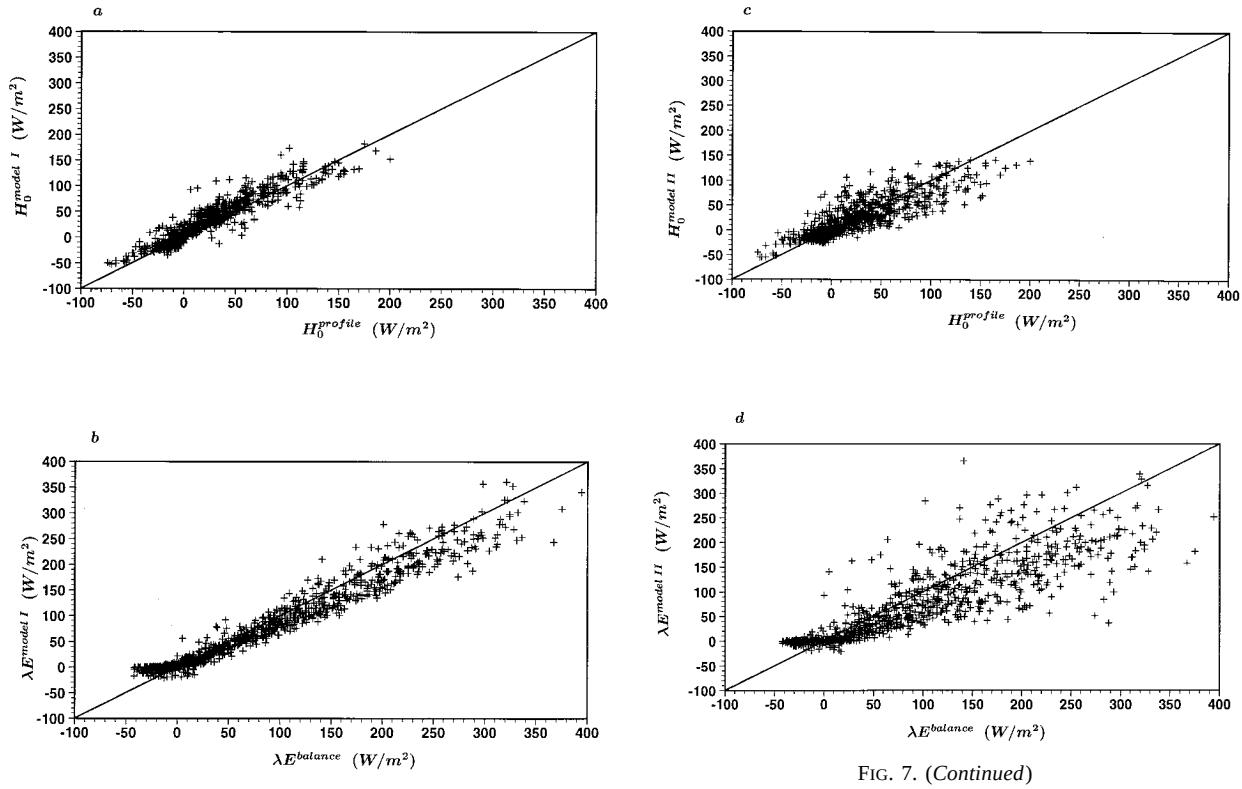

FIG. 7. (*Continued*)

FIG. 7. Comparison of synthetic data with observations for the half hour intervals during which both quantities are available. (a)–(d) Sensible and latent heat fluxes with models I and II for the month of June. (e)–(h) Monthly means of the difference between models I and II and observations of the four components of the surface energy balance.

2) VALIDATION PARAMETERS

For the different components of the surface energy balance, the model by Van Ulden and Holtslag (1985), coded in the so-called FLUXLIB library by Beljaars and Holtslag (1990), is used. The model has empirical formulas for radiation and applies the Priestley–Taylor concept for sensible and latent heat fluxes. It is used for all the components of the surface energy balance (except for the radiation components that are prescribed) in two different ways: (i) with net radiation input from Cabauw (model I) and (ii) with data from De Bilt, including downward solar radiation (model II). The results from model II are always available because the SYNOP station at De Bilt has 100% data coverage—in case of instrument failure, backup instruments are used or interpolation from other stations is applied. The model has been developed and tested with the help of Cabauw data from before 1987, and it was concluded that it gave reasonable results for different applications [see Holtslag and Van Ulden (1983) for daytime fluxes and Holtslag and De Bruin (1988) for nighttime fluxes]. However, these studies concentrated on the diurnal cycle and on the derivation of similarity parameters for diffusion problems. In this paper we consider the long-term averages of the surface energy balance.

A comparison between the profile H_0 and the balance λE on one hand and the models I and II on the other hand is given in Figs. 7a–d as scatterplots for the month of June. It is clear that model I gives better results than model II. The reason is twofold: (i) model I has a less demanding parametrization because it uses net radiation, whereas model II uses solar radiation; and (ii) model I uses local observations of Cabauw, whereas model II uses SYNOP data from 25 km away (De Bilt). The daytime sensible and latent heat fluxes of the two models correlate well with the observations. The nighttime latent heat fluxes from both models have the tendency of leveling off at small negative values, whereas the λE, as derived from the balance method, produces larger negative values. Some of this discrepancy may also be due to the balance method, which seems to overestimate the downward flux by a small amount (see Fig. 5b). Monthly mean differences between the two models and observations are shown in Figs. 7e,h. The model biases of the monthly means are considerable and also have an annual cycle. This is perhaps not a real surprise because the model has never been tested or tuned on monthly averages. The consequences of the impact of these model biases are limited because the percentage of data points replaced by synthetic or model data is small, as we will see in the next section.

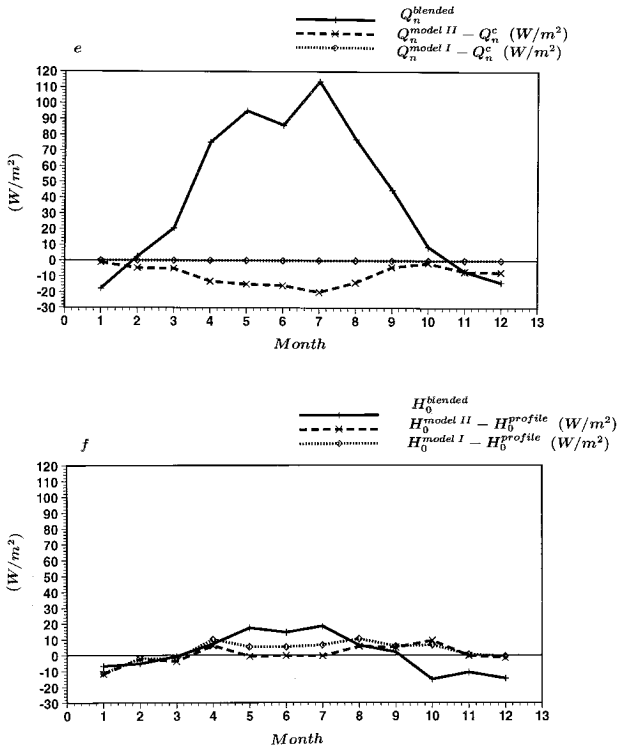

FIG. 7. (*Continued*)

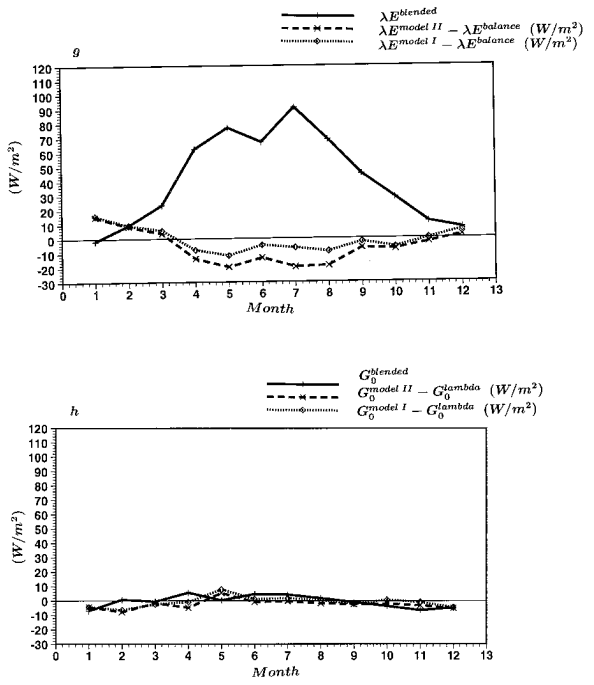

FIG. 7. (*Continued*)

5. Final dataset and error considerations

The final dataset is a blend of observations and data from models I and II. The parameters included in the dataset are listed in Table 4. Every data point has an indicator attached, which can have the value 0, 1, or 2. Indicator value 0 is used for an observation or interpolation between observed values. The indicator values 1 and 2 are used for synthetic data generated with models I and II, respectively. In this way the user can distinguish between real and synthetic data points.

A summary of monthly mean parameters is given in the Figs. 8 and 9. For wind, temperature, specific humidity, and solar downward radiation as well, the observations from De Bilt are shown to give some insight into spatial heterogeneity. Precipitation is compared with the three nearest rain gauge stations. Wind has been ''transformed'' to the Cabauw location to account for exposure differences. Temperature, specific humidity, and wind, transposed from De Bilt to Cabauw, have been extrapolated upward to the level of 20 m with help of surface fluxes of model II and similarity functions.

The percentages of data points from observations and from models I and II are given in Figs. 9b,d,f,h for the four components of the surface energy balance. It is clear that the final data are dominated by observations; the percentage of synthetic data is smaller than 20% for most months.

We now turn to the issue of uncertainty in the data. We distinguish the forcing data and the surface fluxes used for verification. Estimates of uncertainty can only be crude and should be used with caution. Monna and van der Vliet (1987) suggest accuracies of wind and temperature of 1% and 0.1 K, respectively. Specific humidity is derived from dry- and wet-bulb temperatures both with an accuracy of 0.1 K, which leads to a typical error in the specific humidity deficit of 0.3 g Kg^{-1}. Downward solar and thermal radiation have been discussed in section 4b and are believed to be accurate to within a few percent. Precipitation is probably the most difficult observation of all the forcing parameters. It has high spatial variability and serious instrumental difficulties. From the instrumental problems, we distinguish the wind error and the wetting error. The type of electronic rain gauge with a float recorder (with a 0.04-m^2 collector surface area) that was in use at Cabauw in 1987 was compared with a reference rain gauge that has its collector opening flush with the surface. This comparison was made at different locations in the Netherlands (not at Cabauw) by Buishand and Velds (1980) to study the wind error of the instrument. The wind effect results in an underestimation varying between 2% and 11%, dependent on season and location. The coast locations with a windy environment gave the largest error. It is fair to say that the rain gauge at Cabauw is located in very open terrain, and therefore a pronounced wind error is to be expected. A comparison of monthly mean precipitation at Cabauw with three surrounding stations is shown in Fig. 8f. The total precipitation amounts observed in 1987 at Cabauw, Benschop (14 km from Cabauw), Gouda (14 km from Cabauw), and Groot Ammers (9 km from Cabauw) are 772, 859, 903,

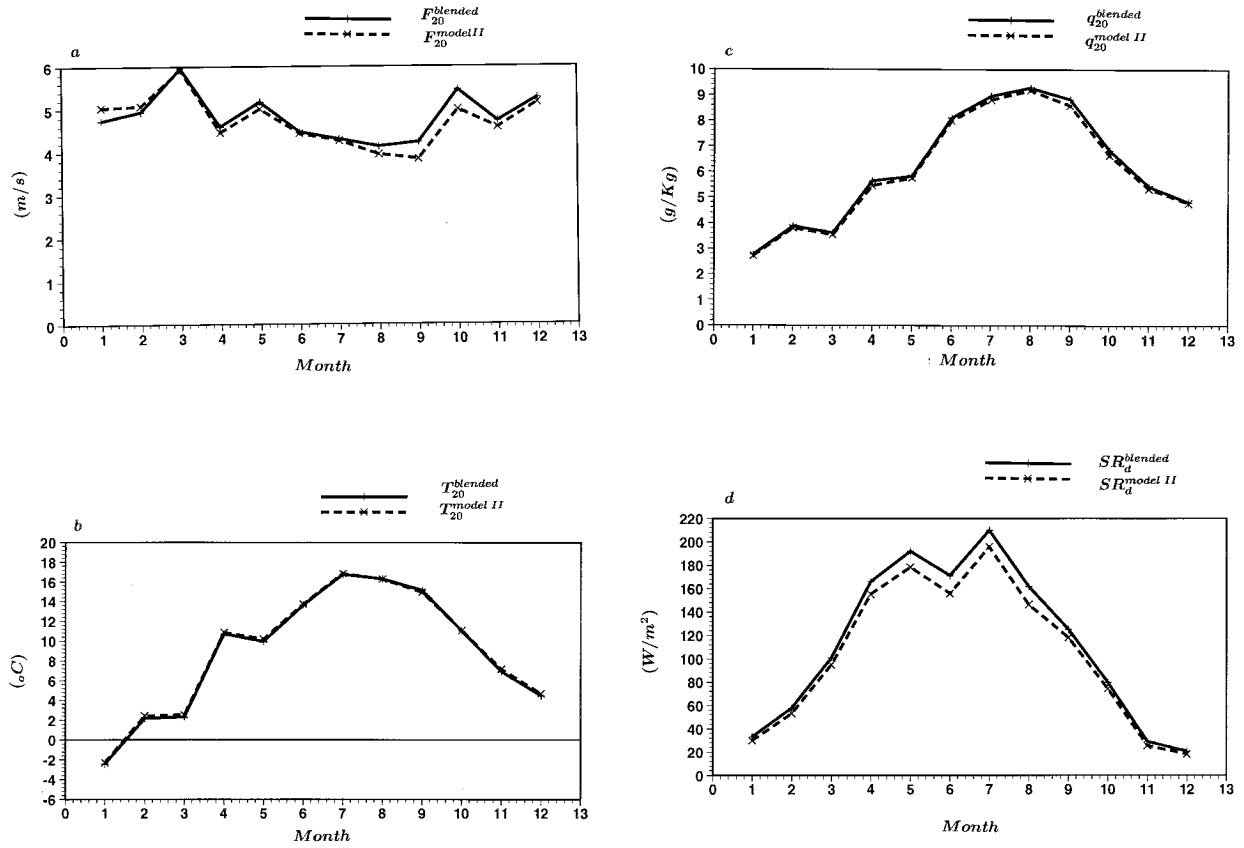

FIG. 8. Monthly means of a selection of parameters in the final blended dataset. (a) Wind at 20-m height at Cabauw (solid) and transposed at De Bilt (dashed). (b) Temperature at 20-m height at Cabauw (solid) and extrapolated from De Bilt (dashed). (c) Specific humidity at 20-m height at Cabauw (solid) and extrapolated from De Bilt (dashed). (d) Solar downward radiation at Cabauw (solid) and at De Bilt (dashed). (e) Downward (solid) and upward (dashed) radiation in Cabauw. (f) Precipitation at Cabauw, at Benschop (6 km from Cabauw), at Gouda (14 km from Cabauw), and at Groot Ammers (9 km from Cabauw).

FIG. 8. (*Continued*)

and 959 mm, respectively. It is difficult to say whether these differences are due to spatial variability or are related to the wind error, but it is likely that the wind error at Cabauw is larger than at the other stations, which would explain the rather systematic difference between Cabauw and the surrounding stations. The so-called wetting loss, due to evaporation from the rain gauge funnel, is estimated by Wammerdam (1981) to be about 3%, but this error applies to all locations and gauge types.

For the monthly mean surface fluxes, the following procedure is followed. Since the final data are a blend of observations and data from models I and II, we first estimate the monthly mean errors of these three components separately and then weigh the errors according to their data coverage (see Table 5). The monthly mean error in the net radiation is estimated from the maximum radiation residual, which is about ± 5 W m^{-2}. For the sensible heat flux from the profile method, we estimated the uncertainty as being ± 2.5 W m^{-2} from the maximum temperature errors. We have no independent way of measuring the ground heat fluxes, but the contribution to the surface energy budget is small, and the errors are likely to be less than 1 W m^{-2}. The latent heat flux has been derived as a residual from the surface energy balance, and therefore the maximum error in the latent heat flux is the sum of the errors in the other components.

For the errors in models I and II, we simply take the maximum monthly mean difference between observation and model (see Table 5). Models I and II have a distinct annual cycle, and therefore the maximum monthly mean error is a safe (over) estimate for most months.

The error of the blended data is calculated as the sum of the errors of the three components weighed with the data coverage for that particular month. The results of this procedure are indicated as the upper and lower bounds in Fig. 9.

6. Evaporation control

One of the main functions of a land surface scheme in a large-scale atmospheric model is to partition the available energy at the surface between sensible and latent heat fluxes. Different models have different levels

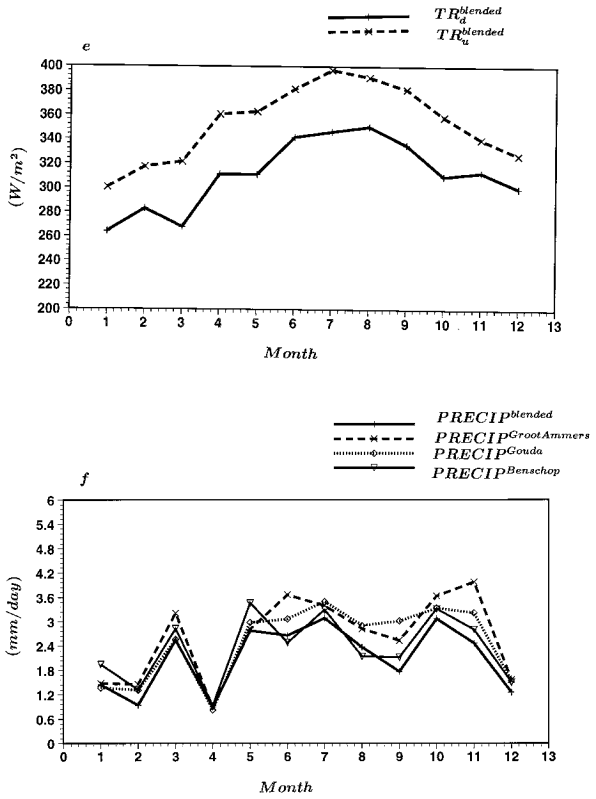

FIG. 8. (*Continued*)

of complexity, but many use a canopy resistance to control the plant transpiration. Additionally, most models consider evaporation from an interception reservoir with zero surface resistance (i.e., controlled by aerodynamic resistance only). Bare ground and snow evaporation are usually also considered, but are less relevant for the Cabauw location because snow cover is not very frequent and the vegetation cover is nearly 100% in all seasons. Therefore, the main aspects of evaporation control are the interception reservoir evaporation and the plant transpiration.

Although difficult to quantify, we know that interception reservoir evaporation is very important at the Cabauw location. The 772 mm of precipitation in 1987 are spread rather uniformly over the year (Fig. 10) and wet the vegetation on the many rainy days. Additionally, dew in the morning (due to dew deposition and/or dew rise) is a very common feature. Because of the high frequency of water on the vegetation, models may be sensitive to the formulation of the aerodynamic resistance, as demonstrated by Beljaars and Viterbo (1995) with a stand-alone simulation of the ECMWF land surface scheme for the 1987 Cabauw data. Their simulated annual interception evaporation is 31% of the total evaporation. It is of course difficult to say how accurate these numbers are, because interception reservoir evaporation has not been measured (and is very difficult to measure for low vegetation).

With regard to transpiration control, we first consider the broad climatological regime, as defined by precipitation and evaporation. On a timescale of a few days, precipitation exceeds or balances evaporation most of the time, and therefore drying out the soil is of secondary importance in 1987, as illustrated by the time-integrated difference between precipitation and evaporation in Fig. 10. The maximum soil moisture depletion is from day 84 to day 195, during which evaporation exceeds precipitation by only 80 mm. If we think of the top soil layer as a reservoir with a water-holding capacity of 150 mm, then the reservoir is only emptied to 47% of its capacity at day 195. With the abundant rain between day 195 and day 210, the water level in the reservoir goes back rapidly to the 73% level.

In order to study the behavior of the vegetation in relation to possible controlling mechanisms, we consider the canopy or surface resistance r_s derived from the Penman–Monteith equation (Monteith 1965). This is the so-called top-down approach, in which the canopy resistance is diagnosed from measurements that are taken well above the vegetation without considering the details of the plant physiology (Baldocchi et al. 1991). The advantage is that we obtain a parameter that is useful for large-scale models, although it may involve not only the moisture flow through the stomata, but also bare soil evaporation. The Penman–Monteith equation reads

$$\lambda E = \frac{S(Q_n + G_0) + \rho C_p dq/r_a}{S + \gamma(1 + r_s/r_a)} \tag{14}$$

and

$$r_a = \frac{k}{u*[\ln(z/z_{0h}) - \Psi_H(z/L)]}, \tag{15}$$

where λE is the latent heat flux from the Bowen method, S is the derivative of the saturation specific humidity curve, Q_n is the observed net radiation, G_0 is the observed ground heat flux, ρ is the air density, C_p is the air heat capacity at constant pressure, dq is the observed moisture deficit ($q_s - q$, with q being specific humidity at the observation height of 20 m and q_s being the saturation value at the observed temperature), r_a is the aerodynamic resistance between the observation level and the surface, r_s is the canopy resistance, k in the von Karman constant, u_* is the observed friction velocity from the profile method, z_{0h} is the roughness length for heat, Ψ_H is the profile stability function for temperature (Beljaars and Holtslag 1991), and L is the Obukhov length from observed fluxes. The roughness length for heat is taken as 0.1 of the roughness length for momentum (see section 3 and Table 3). The latent heat flux from the Bowen method has been selected here because it is believed to be the most accurate one, although the data coverage is less than with the balance method.

The nighttime values for r_s are often small compared to the aerodynamic resistance and are, therefore, inac-

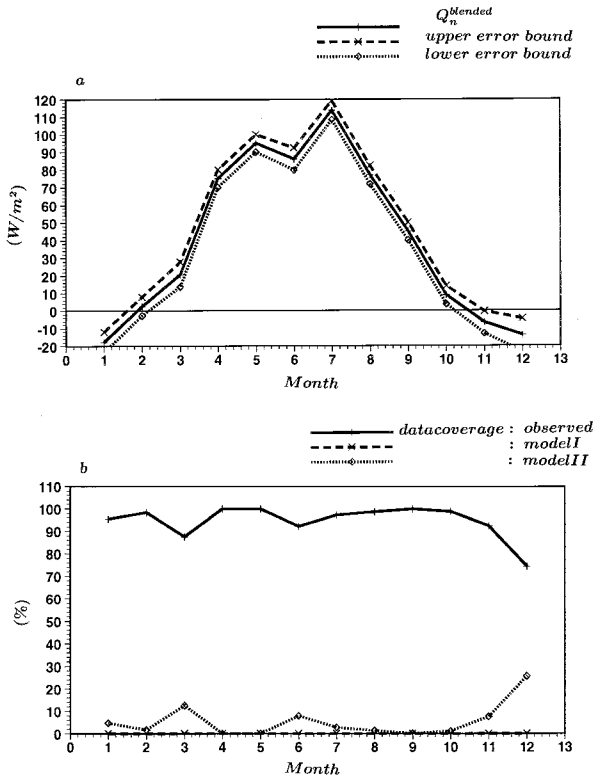

FIG. 9. Monthly means of net radiation, sensible heat flux, latent heat flux, and ground heat flux, with error bounds and coverage by observations and data from models I and II.

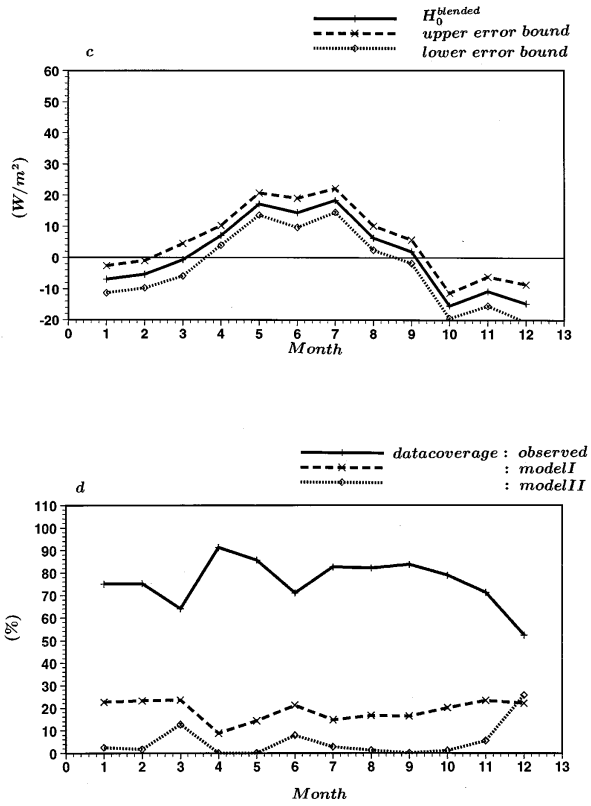

FIG. 9. (*Continued*)

curate and noisy. Thus, we concentrate on the daytime, and we also do so because total evaporation is mainly determined by daytime values. Midday values of r_s are given in Fig. 11a as a time series for the entire year. Results are only plotted if the observations to compute r_s are available, so no synthetic data are used here. The mean daytime evolution of r_s is given for the month of June in Fig. 11b.

Although ample soil water is available most of the time, it does not imply that the surface resistance is constant. Some of the variability may be due to experimental noise, but most of the variability is believed to be related to ''environmental conditions.'' For instance, the drying period between day 180 and day 195 shows a clear increase of the midday canopy resistance, and the period with abundant precipitation just after that coincides with a pronounced drop in the resistance. In addition, the increase of r_s during the day is very pronounced and is observed throughout the year.

Parameters that potentially influence the surface resistance are water on the vegetation ($r_s = 0$), soil water availability, photoactive radiation (PAR), air temperature, and air moisture deficit. Unfortunately, vegetation wetness and soil water availability were not measured. PAR was not measured either, but we will assume that PAR is proportional to the solar downward radiation. To get an estimate of the wetness of the vegetation and

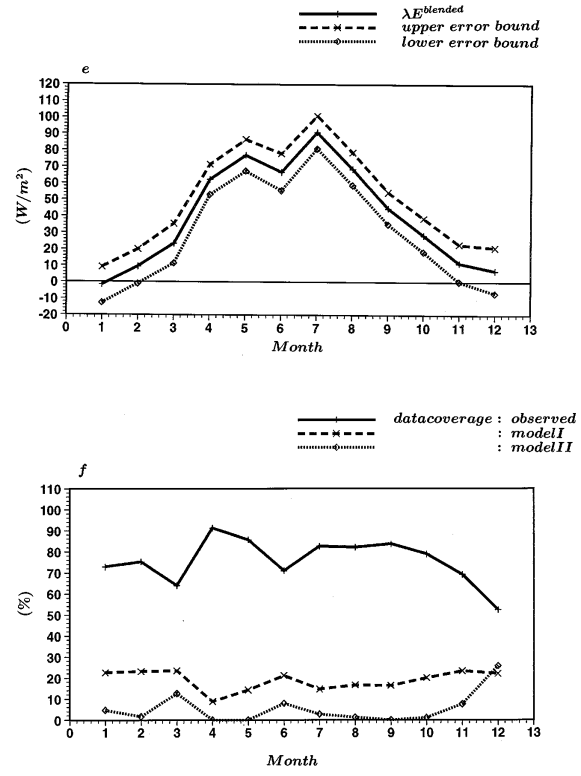

FIG. 9. (*Continued*)

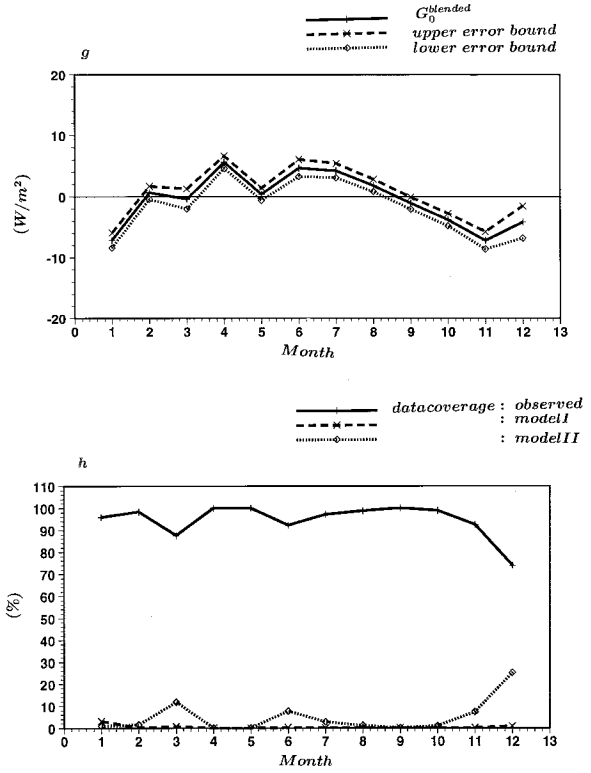

FIG. 9. (*Continued*)

the soil water availability, we will use the output of the stand-alone simulation with the ECMWF land surface scheme, as produced by Viterbo and Beljaars (1995) for the Cabauw data. These are not real data of course, but we will use the model interception reservoir content only as part of a selection procedure to isolate data with dry vegetation. For soil water availability, we also use the model output because it is believed to be better than the integrated difference between precipitation and evaporation. The model also includes gravitational drainage and saturation runoff, and therefore automatically deletes excess water when precipitation exceeds evaporation systematically. Diurnal averages of model interception water content and the volumetric soil water content averaged over the two topsoil layers (0.07 + 0.21 m) are displayed in the Fig. 12. The seasonal variation of the modeled soil water in the root zone (28 cm) is weak (as expected), except between day 180 and day 195, when some drying occurs.

We now select dry canopy only to study the behavior of the canopy resistance. The following conditions are used: (i) $SR_d > 5$ W m^{-2} (i.e., daytime only), (ii) no rain, (iii) an empty interception reservoir in the ECMWF model, and (iv) a moisture deficit at 20-m height larger than 1 g kg^{-1}. The data selection reduces the amount of data to 2109 half hour values and changes the evolution of r_s, as can be seen in Fig. 11. The systematic increase of r_s in the morning hours in Fig. 11 has become less pronounced with the selection of dry vegetation,

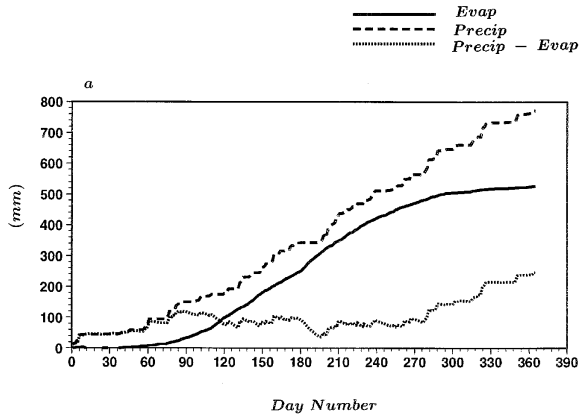

FIG. 10. Accumulated precipitation, evaporation, and difference during 1987.

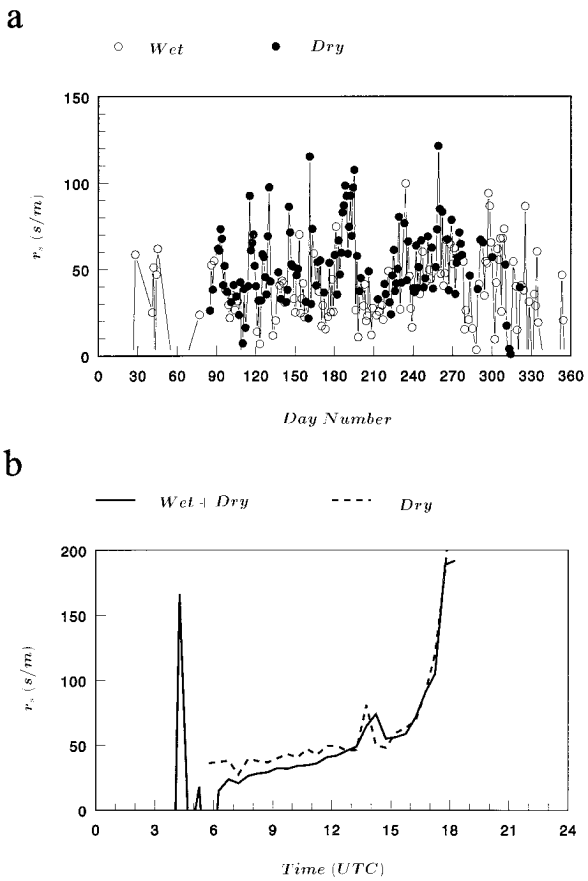

FIG. 11. Time series of midday averages of (a) canopy resistance and (b) its mean diurnal evolution for the month of June. In (a) the closed symbols represent dry vegetation; open symbols are used for the remaining data. In (b) the solid line represents all data, and the dashed line represents dry vegetation only. The Bowen method has been used without inclusion of synthetic data.

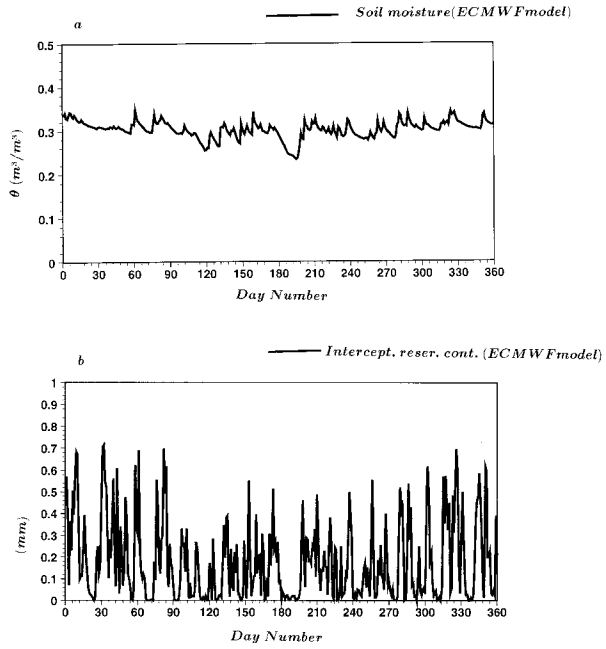

FIG. 12. (a) Time series of diurnal averages of volumetric soil water content of the top-28-cm soil layer and (b) the content of the interception reservoir from the stand-alone simulation with the ECMWF land surface scheme.

and the diurnal pattern has become less asymmetric. It is interesting that dry vegetation results do not suggest any seasonal evolution of r_s.

The observed resistances for dry vegetation are very similar in magnitude and diurnal evolution to the ones observed by Kohsiek (1981) with the help of an evaporation chamber at the Cabauw site. He used the chamber at different locations on the measuring field and also made observations at one of the surrounding fields with long grass and different grass species. The observed canopy resistances were very similar, which suggests that r_s does not depend very strongly on the leaf area index at Cabauw.

The bulk canopy resistance is often modeled as a product of reduction functions (Jarvis 1976; Stewart 1988). It is assumed that the environmental factors that influence r_s are leaf area index, specific humidity deficit dq, solar radiation SR_d, and volumetric soil water content in the root zone. The dependence on air temperature was tried initially, but was dropped because of its strong correlation with moisture deficit and solar radiation. The following formulation is used:

$$r_s = \frac{r_{s,\min}}{f_q(dq)\, f_{SR}(\mathrm{SR}_d)\, f_\theta(\theta)}, \tag{16}$$

with a soil moisture response function (θ is the volumetric soil moisture in the root zone)

$$\begin{aligned} f_\theta(\theta) &= 1 && \text{for } \theta > \theta_{\mathrm{fcp}}, \\ f_\theta(\theta) &= 1 + c_{\mathrm{soil}}(\theta - \theta_{\mathrm{fcp}}) && \text{for } \theta < \theta_{\mathrm{fcp}}, \\ \theta_{\mathrm{fcp}} &= 0.3, \end{aligned} \tag{17}$$

a moisture deficit function (Lohammar 1980)

$$f_q(dq) = \frac{1}{1 + a_q(dq - dq_r)}, \qquad dq_r = 3 \text{ g kg}^{-1}, \tag{18}$$

and a light response function (equivalent to the ones used by Jarvis 1976; Stewart 1988)

$$f_S(\mathrm{SR}_d) = \frac{\mathrm{SR}_d(\mathrm{SR}_m - \mathrm{SR}_{1/2})}{\mathrm{SR}_d \mathrm{SR}_m + \mathrm{SR}_{1/2}(\mathrm{SR}_m - 2\mathrm{SR}_d)}, \qquad \mathrm{SR}_m = 1000 \text{ W m}^{-2}. \tag{19}$$

There is obviously some arbitrariness in the selected formulations, but the free parameters $r_{s,\min}$, a_q, c_{soil}, and $\mathrm{SR}_{1/2}$ give sufficient freedom to optimize the fit of r_s to the observations.

Two different models with the Penman–Monteith equation (PM) are considered using different degrees of freedom in the stress functions. Model 1 uses the PM with $f_S = 1$, $f_q = 1$, and optimal $r_{s,\min}$ and c_{soil}. Model 2 uses the PM with optimal $SR_{1/2}$, a_q, $r_{s,\min}$, and c_{soil}.

Because of its simplicity, we will also consider the Priestley–Taylor formulation (PT) in the form used by De Bruin and Holtslag (1982), which we call model 3:

$$\lambda E = \alpha f_\theta(\theta) \frac{Q_n - G_0}{1 + \gamma/S} + \beta. \tag{20}$$

Model 3 uses the PT with optimal α, β, and c_{soil}.

The three models have been optimized for the selected data, and the optimal coefficients are given in Table 6.

TABLE 5. Error estimates of monthly means of the four components of the surface energy balance in W m^{-2}. Observations and model results are distinguished.

	Observations	Model I	Model II
Q_n	±5	(Not used)	±22
H_0	±2.5	±10	±10
λE	±7.5	±16	±23
G_0	±1	± 8	± 8

TABLE 6. Optimal coefficients for models 1, 2, and 3.

Model	Parameter	Optimal value	Units
Model 1 (Penman–Monteith)	$r_{s,\min}$	39.2	s m^{-1}
$\sigma\lambda E$ = 23.6 W m^{-2}	c_{soil}	9.0	m^3 m^{-3}
Model 2 (Penman–Monteith)	$r_{s,\min}$	25.9	s m^{-1}
$\sigma\lambda E$ = 20.1 W m^{-2}	c_{soil}	6.3	m^3 m^{-3}
	a_q	0.16	kg g^{-1}
	$\mathrm{SR}_{1/2}$	230	W m^{-2}
Model 3 (Priestley–Taylor)	α	1.05	
$\sigma\lambda E$ = 21.2 W m^{-2}	β	24	W m^{-2}
	c_{soil}	1.1	m^3 m^{-3}

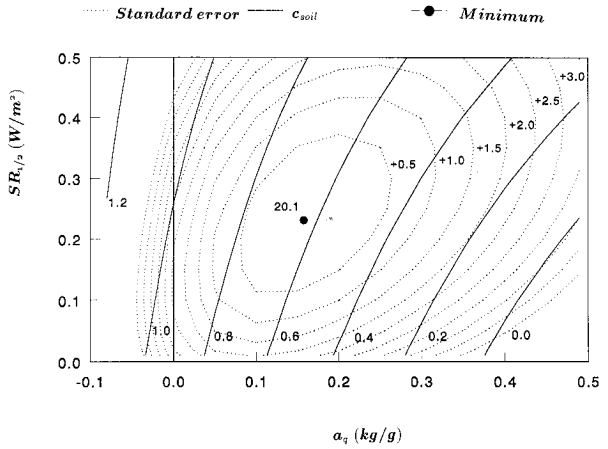

FIG. 13. Contour plot of the standard error in λE (dotted), with model 2 as a function of parameter $SR_{1/2}$ and c_q with optimal values for c_{soil} and $r_{s,min}$. The corresponding optimal c_{soil} values are drawn as solid contours.

Model 2, which is the most complicated, gives the best results, with a standard deviation of the residual between the modeled and observed latent heat fluxes of 20.1 W m^{-2}. The second best is model 3, with a standard error of 21.2, while model 2 has an standard error of 23.6 W m^{-2}. It is clear that all three models do a reasonable job on the dataset as a whole and that more degrees of freedom give a better fit to the data. To gain more insight in the sensitivity to parameter values, a contour plot is given of the standard deviation of the residual of latent heat flux as a function of $SR_{1/2}$ and a_q for model 2, with c_{soil} and $r_{s,min}$ optimized (Fig. 13). The optimal values of c_{soil} are also drawn. An increase of only 0.5 W m^{-2} of the residual allows for quite a large change in the parameters of the stress functions, so the estimates of the parameters are rather crude.

However, inspection of the mean residuals of the three models as functions of time of the day and moisture deficit illustrate the weak and strong aspects of the different models (Figs. 14a,b). Model 3 does a remarkably good job on the diurnal cycle, which suggests that the diurnal cycle of the latent heat flux follows that of the available energy ($Q_n - G_0$) very closely. The deviation of model 1 from the observations has a distinct diurnal cycle with too much latent heat flux in the early morning, too little before noon, and too much in the afternoon. The reason is the lack of a solar radiation and moisture deficit dependence in the stress functions. Model 2, with all the stress functions, performs similarly to model 3.

The residuals shown as a function of moisture deficit in Fig. 14b indicate an underestimation with model 3, an overestimation with model 1, and virtually no bias with model 2. The difference between models 1 and 2 and model 3 is the moisture deficit term of the Penman–Monteith equation, which is not present in the Priestley–Taylor formulation. The Priestley–Taylor formulation

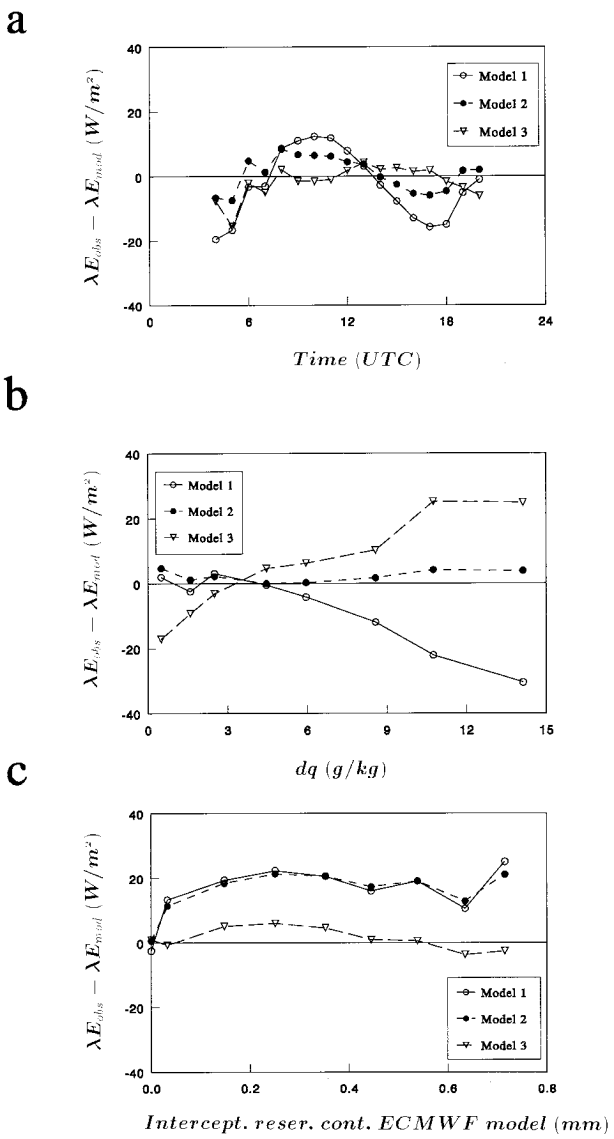

FIG. 14. Mean error in λE, with models 1, 2, and 3 as functions of (a) time of the day, (b) moisture deficit dq, and (c) interception reservoir content of the ECMWF model. In (a) and (b) the selected dry vegetation is data used; (c) includes all data.

cannot simulate the additional evaporation in dry air, but a simple Penman–Monteith equation without a $f_q(dq)$ function overestimates the effect of the moisture deficit term. Only with additional control on the canopy resistance, as in model 2, are unbiased latent heat fluxes produced.

So far we have concentrated on the dry vegetation, but to see the effect of wet vegetation we drop the condition of zero water content in the interception reservoir of the ECMWF model simulation. The bias of the three models is shown in Fig. 14c as a function of the interception reservoir content. As expected, models 1 and 2 underestimate the evaporation because they do not reproduce the low canopy resistance in case of wet

vegetation. However, model 3 does a remarkable job for reasons that are not obvious. Apparently, the effect of the moisture deficit term in the Penman–Monteith equation correlates strongly with the $Q_n - G_0$ term, which means that they can be captured with one single term, as in the Priestley–Taylor formulation.

Two conclusions emerge from this analysis. First, evaporation from the interception reservoir is an important mechanism, and wet vegetation occurs frequently throughout the year due to rain, but also due to deposition of dew and/or dew rise (distillation). Second, the canopy resistance needs a series of control functions in order to give reasonable behavior in the Penman–Monteith equation. It was surprising to see that the rather empirical Priestley–Taylor formulation, with three optimized coefficients, gives a similar fit to the data. Apparently, the moisture deficit term and the available energy term in the Penman–Monteith equation are highly correlated (De Bruin and Holtslag 1982).

7. Concluding remarks

A dataset has been presented that can be used for the validation of land surface schemes. It includes forcing data to drive such schemes in stand-alone mode and surface fluxes for comparison with their output. The data represent a full year of observations, with emphasis on the seasonal timescale. A firm estimate of the accuracy of the monthly means is difficult to make. By looking at consistency between different instruments and by looking at different methods to derive sensible and latent heat fluxes from the observations, a crude estimate has been made. It is believed that the monthly means of the sensible heat fluxes are within ± 5 W m^{-2} the net radiation is within ± 10 W m^{-2}, and the latent heat flux is within ± 10 W m^{-2}.

The control of evaporation by environmental factors has been investigated by optimizing parameters in the formulation of the bulk canopy resistance of the Penman–Monteith formula and by optimizing parameters in the Priestley–Taylor approach. It became clear that wetness of the vegetation was a very important factor, particularly in 1987, which was rather gloomy and rainy with precipitation spread uniformly over the entire year. Thus, interception reservoir modeling is certainly an important aspect of a land surface scheme being used in this dataset. To study the stomatal control, dry periods were selected and stress functions were optimized. It can be concluded that radiation control, soil moisture control, and control by moisture deficit are all necessary to obtain a good simulation in all situations. Although slightly inferior to the Penman–Monteith formulation (including all the stress functions), the Priestley–Taylor approach works surprisingly well. Its diurnal cycle is very good, and the model works even when the vegetation is wet, although evaporation is underestimated for large values of the moisture deficit. The fact that the Priestley–Taylor formulation works so well implies that the fraction of energy used for evaporation [$\lambda E/(Q_n - G_0)$] is a very robust parameter. It shows much less variation than the canopy resistance. If a canopy resistance is used, it is necessary to control it with moisture deficit and solar radiation. This conclusion only applies to the daytime situation because the relation between available energy and latent heat flux is completely different at night.

This dataset corresponds to a climatological regime in which drying out of the soil is of secondary importance. This is illustrated by the time-integrated difference between precipitation and evaporation and by a simulation with a state-of-the-art land surface scheme. Soil moisture stress is limited to a short period of time only.

Acknowledgments. Long-term monitoring of boundary layer parameters such as that done at Cabauw is a team effort. Over the years, it has involved many people at the Royal Netherlands Meteorological Institute, and we would like to acknowledge their efforts. In particular, we would like to thank Bert Holtslag for his encouragement to initiate this project, and Adri Buishand, Wim Kohsiek, and Gerard van der Vliet for their help in solving data problems. Wim Bastiaansen from the Winand Staring Centre helped find and interpret the information on soil characteristics, and Michael Ek helped organize our thoughts through lengthy discussions during the preparation of the manuscript.

Many of the issues discussed in this paper are the result of questions asked by the PILPS team after the models were run. The quality control and the documentation of the measuring site benefited considerably from the feedback provided by the PILPS team. Tian Chen and Sam Chang experimented with an early version of the revised data and gave valuable suggestions for improvement of the manuscript and the processing of data.

REFERENCES

Abramopoulos, F., C. Rosenzweig, and B. Choudhury, 1988: Improved ground hydrology calculations for global models (GCMs): Soil water movement and evapotranspiration. *J. Climate,* **1,** 921–941.

André, J. C., J. P. Goutorbe, and A. Perrier, 1986: HAPEX/MOBILHY: A hydrologic atmospheric experiment for the study of water budget and evaporation flux at the climatic scales. *Bull. Amer. Meteor. Soc.,* **67,** 138–144.

Baldocchi, D. B., R. J. Luxmoore, and J. L. Hatfield, 1991: Discerning the forest from the trees: An essay on scaling canopy stomatal conductance. *Agric. For. Meteor.,* **54,** 197–226.

Beljaars, A. C. M., 1982: The derivation of fluxes from profiles in perturbed areas. *Bound.-Layer Meteor.,* **24,** 35–55.

——, 1988: The measurements of gustiness at routine wind stations. *WMO Tech. Conf. on Instruments and Methods of Computation,* Leipzig, Germany, World Meteor. Org., 311–316.

——, and A. A. M. Holtslag, 1990: A software library for the calculation of surface fluxes over land and sea. *Environ. Software,* **5,** 60–68.

——, and ——, 1991: On flux parametrization over land surfaces for atmospheric models. *J. Appl. Meteor.,* **30,** 327–341.

——, and P. Viterbo, 1994: The sensitivity of winter evaporation to the formulation of aerodynamic resistance in the ECMWF model. *Bound.-Layer Meteor.,* **71,** 135–149.

——, P. Schotanus, and F. T. M. Nieuwstadt, 1983: Surface layer similarity under nonuniform fetch conditions. *J. Climate Appl. Meteor.,* **22,** 1800–1810.

Bolle, H. J., and Coauthors, 1993: EFEDA: European Field Experiment in a Desertification Threatened Area. *Ann. Geophys.,* **11,** 173–189.

Buishand, T. A., and C. A. Velds, 1980: *Neerslag en Verdamping.* Koninklijk Nederlands Meteorologisch Instituut, 206 pp.

Chen, T. H., and Coauthors, 1997: Cabauw experimental results from the Project for Intercomparison of Land-surface Parameterization Schemes (PILPS). *J. Climate,* **10,** 1194–1215.

Deardorff, J. W., 1978: Efficient prediction of ground surface temperature and moisture, with inclusion of a layer of vegetation. *J. Geophys. Res.,* **83,** 1889–1903.

De Bruin, H. A. R., and A. A. M. Holtslag, 1982: A simple parameterization of the surface fluxes of sensible and latent heat during daytime compared with the Penman–Monteith concept. *J. Appl. Meteor.,* **21,** 1610–1621.

De Vries, D. A., 1963: Thermal properties of soil. *Physics of Plant Environment,* W. R. Van Wijk, Ed., North Holland Publishing, 210–235.

Dickinson, R. E., A. Henderson-Sellers, P. J. Kennedy, and M. F. Wilson, 1986: Biosphere–Atmosphere Transfer Scheme (BATS) for the NCAR community model. NCAR Tech. Note NCAR/TN-275+STR, 69 pp. [Available from National Center for Atmospheric Research, P.O. Box 3000, Boulder, CO 80307.]

Duynkerke, P. G., 1992: The roughness length for heat and other vegetation parameters for a surface of short grass. *J. Appl. Meteor.,* **31,** 579–586.

Garratt, J. R., 1993: Sensitivity of climate simulations to land-surface and atmospheric boundary-layer treatments—A review. *J. Climate,* **6,** 419–449.

——, and R. J. Francey, 1978: Bulk characteristics of heat transfer in the unstable, baroclinic atmospheric boundary layer. *Bound.-Layer Meteor.,* **15,** 399–421.

Halldin, S., and A. Lindroth, 1992: Errors in net radiometry: Comparison and evaluation of six radiometer designs. *J. Atmos. Oceanic Technol.,* **9,** 762–782.

Henderson-Sellers, A., Z.-L. Yang, and R. E. Dickinson, 1993: The project for Intercomparison of Land-Surface Parameterization Schemes. *Bull. Amer. Meteor. Soc.,* **74,** 1335–1349.

——, A. J. Pitman, P. K. Love, P. Irannejad, and T. Chen, 1995: The Project for Intercomparison of Land Surface Parameterization Schemes (PILPS): Phases 2 and 3. *Bull. Amer. Meteor. Soc.,* **76,** 489–503.

Henning, D., 1989: *Atlas of the Surface Heat Balance of the Continents.* Gebrüder Borntraeger, 402 pp.

Hillel, D., 1982: *Introduction to Soil Physics.* Academic Press, 364 pp.

Holtslag, A. A. M., and A. P. Van Ulden, 1983: A simple scheme for daytime estimates of the surface fluxes from routine weather data. *J. Climate Appl. Meteor.,* **22,** 517–529.

——, and H. A. R. De Bruin, 1988: Applied modeling of the nighttime surface energy balance over land. *J. Appl. Meteor.,* **27,** 689–704.

Jager, C. J., T. C. Nakken, and C. L. Palland, 1976: *Bodemkundig Onderzoek van twee Graslandpercelen Nabij Cabauw* (in Dutch). NV Heidemaatschappij Beheer, 9 pp.

Jarvis, P. G., 1976: The interpretation of the variations in leaf water potential and stomatal conductance found in canopies in the field. *Philos. Trans. Roy. Soc. London, Ser. B,* **273,** 593–610.

Kim, J., and S. B. Verma, 1991: Modeling canopy stomatal conductance in a temperate grassland ecosystem. *Agric. For. Meteor.,* **55,** 149–166.

Kohsiek, W., 1981: A rapid-recirculation chamber for measuring bulk stomatal resistances. *J. Appl. Meteor.,* **20,** 42–52.

Lohammar, T., S. Larsson, S. Linder, and S. O. Falk, 1980: FAST-simulation models of gaseous exchange in Scots Pine; Structure and function of northern coniferous forests—An ecosystem study. *Ecol. Bull.,* **32,** 505–523.

Manabe, S., 1969: Climate and the ocean circulation. Part 1: The atmospheric circulation and the hydrology of the earth's surface. *Mon. Wea. Rev.,* **97,** 739–774.

Monna, W. A. A., and J. G. Van Der Vliet, 1987: Facilities for research and weather observations on the 213 m tower at Cabauw and at remote locations. KNMI Scientific Rep. WR-87-5, 27 pp. [Available from Royal Netherlands Meteorological Institute, P.O. Box 3730AE, De Bilt, the Netherlands.]

Monteith, J. L., 1965: Evaporation and environment. *Symp. Soc. Exp. Biol.,* **XIX,** 205–234.

Nieuwstadt, F. T. M., 1978: The computation of the friction velocity u* and the temperature scale T* from temperature and wind profiles by least-square methods. *Bound.-Layer Meteor.,* **14,** 235–246.

Noilhan, J., and S. Planton, 1989: A simple parameterization of land surface processes for meteorological models. *Mon. Wea. Rev.,* **117,** 536–549.

Saugier, B., and E. A. Ripley, 1978: Evaluation of the aerodynamic method of determining fluxes over natural grassland. *Quart. J. Roy. Meteor. Soc.,* **104,** 257–270.

Sellers, P., Y. Mintz, Y. C. Sud, and A. Dalcher, 1986: A Simple Biosphere Model (SiB) for use with general circulation models. *J. Atmos. Sci.,* **43,** 505–531.

——, F. G. Hall, G. Asrar, D. E. Strebel, and R. E. Murphy, 1988: The First, ISLSCP Field Experiment (FIFE). *Bull. Amer. Meteor. Soc.,* **69,** 22–27.

Shuttleworth, W. J., and Coauthors, 1984: Eddy correlation measurements of energy partition for Amazonian forest. *Quart. J. Roy. Meteor. Soc.,* **110,** 1143–1162.

Slob, W. M., 1978: The accuracy of aspiration thermometers. KNMI Scientific Rep. WR 78-1, 17 pp. [Available from Royal Netherlands Meteorological Institute, P.O. Box 3730AE, De Bilt, the Netherlands.]

Stewart, J. B., 1988: Modeling surface conductance of pine forest. *Agric. For. Meteor.,* **43,** 19–35.

van Genuchten, M. T., 1980: A closed-form equation for predicting the hydraulic conductivity of unsaturated soils. *Soil Sci. Soc. Amer. J.,* **44,** 892–898.

van Ulden, A. P., and A. A. M. Holtslag, 1985: Estimation of atmospheric boundary layer parameters for diffusion applications. *J. Climate Appl. Meteor.,* **24,** 1196–1207.

——, and J. Wieringa, 1996: Atmospheric boundary layer research at Cabauw. *Bound.-Layer Meteor.,* **78,** 39–69.

Vermetten, A. W. M., L. Ganzeveld, A. Jeuken, P. Hofschreuder, and G. M. J. Mohren, 1994: CO_2 uptake by a stand of Douglas fir: Flux measurements compared with model calculations. *Agric. For. Meteor.,* **72,** 57–80.

Viterbo, P., and A. C. M. Beljaars, 1995: An improved land surface parametrization scheme in the ECMWF model and its validation. *J. Climate,* **8,** 2716–2748.

Wammerdam, P. M. M., 1981: De invloed van de wind op regenwaarnemingen; een vergelijkend regenmeteronderzoek. *H_2O,* **14,** 16–20.

Wieringa, J., 1986: Roughness-dependent geographical interpolation of surface wind speed averages. *Quart. J. Roy. Meteor. Soc.,* **112,** 867–889.

Wofsy, S. C., M. L. Goulden, J. W. Munger, S.-M. Fan, P. S. Bakwin, B. C. Daube, S. L. Bassow, and F. A. Bazzaz, 1993: Net exchange of CO_2 in a mid-latitude forest. *Science,* **260,** 1314–1316.

Wösten, J. H. M., G. J. Veerman, and J. Stolte, 1994: Waterretentie- en doorlatendheid-skarakteristieken van boven- en ondergrond in Nederland: De Staringreeks (in Dutch). Tech. Document 18, 66 pp. [Available from Winand Staring Centre for Integrated Land, Soil and Water Research, P.O. Box 125, 6700AC, Wageningen, the Netherlands.]